MARTIAN ENVIRONMENTAL EFFECTS ON SOLAR CELLS AND SOLAR CELL COVER GLASSES

Prepared for

Jet Propulsion Laboratory
4800 Oak Grove Drive
Pasadena, California
Attention: M. Beckstrom

Contract No. 952582

TTU Report 3101 - Final

1 August 1971

Prepared by

F. Alton Wade
Principal Investigator
Department of Geosciences
Texas Tech University
Lubbock, Texas

MARTIAN ENVIRONMENTAL EFFECTS ON SOLAR CELLS AND SOLAR CELL COVER GLASSES

Prepared for

Jet Propulsion Laboratory
4800 Oak Grove Drive
Pasadena, California
Attention: M. Beckstrom

Contract No. 952582

TTU Report 3101 - Final

1 August 1971

Prepared by

F. Alton Wade
Principal Investigator
Department of Geosciences
Texas Tech University
Lubbock, Texas

ABSTRACT

This report presents the results of a study concerned with the effects of the Martian environment on the performance of solar cells. This study was performed by Texas Tech University for the Jet Propulsion Laboratory, Pasadena, California, under Contract 952582, a subcontract of NASA, NAS7-100.

The results of this study indicate that the efficiency of a power system composed of solar cells will be greatly reduced when subjected to dust storms such as may occur on Mars. Two factors are responsible for this, (1) accumulation of dust on the protective covers, and (2) damage to covers by pitting, cracking, and chipping.

It is recommended that this type of power system not be used on Mars landing vehicles. Experimental procedures are described and results are summarized and damage assessed.

SUMMARY

This report is concerned with the effect of "dust storms" on the operation of solar cell assemblages at or near the surface of Mars.

Included in the NASA space program are landings of space vehicles on Mars. Various scientific experiments are to be performed by remote control and the results transmitted back to Earth by radio and television. A possible source of power to operate the various pieces of equipment and apparatus is the solar cell which has operated most efficiently in outer space and on the Moon. Would the Martian environment have a detrimental effect on its operation? It was believed that if subjected to dust storms the efficiency of the solar cell might be reduced permanently through damage to the assemblage or to the cover glasses. To determine this was the principal objective of this project.

A series of tests was run under simulated Martian environmental conditions to determine the effects of dust storms on the operational efficiency of solar cells. Tests were conducted in wind tunnels in which temperature, wind velocity,

and atmospheric composition could be controlled. In all tests the atmosphere consisted of CO_2 gas in which there was a trace of water vapor. Tests were conducted in six different environments: ambient temperature, 245°K, and a diurnal cycle of 210°K-305°K; all three with wind velocity of 50 km/hr. and then with wind velocity of 100 km/hr. A test was run over a period of 24 hours and then repeated over a 72 hour interval. Dust particles were of two sizes: <60 microns and 125-250 microns.

Four types of cover glasses were tested: Corning No. 0211 microsheet, fused silica, sapphire, and integral. Two types of electrical interconnectors were tested: silver mesh and JPL bus bar. Output of solar cell modules under standardized light conditions was measured and the changes in the operational efficiency due to dust cover and damage to the assemblages determined. Damage to cover glasses and the assemblage was determined by microscopic examinations.

In all six environments dust accumulated on all types of modules almost instantaneously. Reduction in power output due to accumulation of dust on modules and damage ranged between 60% and 80%. Permanent damage was responsible for reduction of power output of from 25% to 40%.

Damage to cover glasses caused by particle impact varied with the material. Sapphire cover glasses were the least effected and in order of increasing damage: integral, fused silica, and microsheet. Unbonding of sapphire and microsheet cover glasses was considerable.

From the experimental results it is concluded that the efficiency of the solar cell as a power generator will be greatly reduced if subjected to dust storms on the Martian surface. Coatings of dust adhere tightly to the surfaces following a dust storm and reduce the incoming solar radiation. In the event that dust did not adhere to the cover glasses in the true Martian environment as it did in the test experiments, the damage to the protective cover glasses on the solar cells would be sufficiently great to reduce the efficiency of the cells and perhaps destroy them.

It is recommended that a source of power other than solar cells be used on space vehicles which are to be landed on Mars. It is recognized that destructive dust storms are of infrequent occurrence on Mars and that in all probability no such storm would occur during a period of experimentation following a soft landing of a space vehicle. However, the possibility of a severe dust storm occuring during that time interval does exist and that project

failures might result. It is further recommended that all equipment which is to be operated on the Martian surface be protected against damage in vulnerable areas from dust storms.

The results of this project prove the vulnerability of solar cells to wind-driven particulate matter. They should not be used as a source of power on a vehicle landed on Mars. Failure of the power source could eliminate the data gathering ability of any equipment. Because of the multimillion dollar cost of the overall project, no chance should be taken which might result in power failure.

CONTENTS

1. INTRODUCTION 1

1.1 Purpose of Investigation 1

2. CONDITIONS AND DESIGN OF EXPERIMENTS 3

2.1 Simulated Martian Environment 3

2.2 Particulate Matter 3

2.3 Descriptions of Wind Tunnels 6

2.4 Solar Cell Assemblages and Solar Cell Cover Glasses 9

2.5 Experimental Program 10

3. DUST COATINGS ON SOLAR CELLS 13

3.1 Development of Dust Coatings 13

3.2 Description of Dust Coatings 13

3.3 Removal of Dust Coatings 16

4. PERMANENT DAMAGE TO SOLAR CELLS AND COVER GLASSES 18

4.1 Summary 18

4.2 Pitting of Surfaces by Wind-driven Particles 19

4.2.1 Corning No. 0211 Microsheet 20

4.2.2 Fused SiO_2 21

4.2.3 Sapphire 21

4.2.4 Integral 22

4.3 Cracking and Chipping of Cover Glasses 22

4.3.1 Corning No. 0211 Microsheet 23

4.3.2 Sapphire 23

4.3.3 Fused SiO_2 24

4.4 Unbonding of Cover Glasses 24

4.5 Failure of Electrical Interconnections 33

4.6 Analysis of Damage Data 33

4.7 Conclusions 35

5. SOLAR CELL OUTPUTS 55

5.1 Introduction 55

5.2 Source of Illumination 55

5.3 Adjustment of the Illumination Source to Simulate the Solar Environment at Mars 56

5.4 Measurement of Solar Cell Ampere-Volt Characteristics 57

5.5 Power Output Data 58

6. SUMMARY, CONCLUSIONS, AND RECOMMENDATIONS 93

6.1 Summary and Conclusions 93

6.2 Recommendations 96

References 97

ILLUSTRATIONS

2-1	Diagram of Wind Tunnel	8
2-2	Program of Testing	12
3-1	Solar Cell Assemblage Before Dust Blasting	14
3-2	Solar Cell Assemblage with Thin Layer of Dust Which was Deposited During "Dust Storm" of 24 Hours, 100 km/hr., Ambient Temperature	14
3-3	Four Solar Cell Assemblages Which Had Been Subjected to Same Dust Storm. Note Similarities of Dust Coatings	15
4-1	The Corning No. 0211 Microsheet Cover Glasses Were Free of Surface Imperfections Before Subjecting Them to Dust Storms	25
4-2	Corning Microsheet Cover Glass After Dust Blasting 24 Hours, 50 km/hr., 245°K. Note the Background of Fine Pits and the Scattered Medium- and Large-Size Pits	25
4-3	Same as Figure 4-2, But of Different Area. Note Crater-like Pits and One Radiating Pit	26
4-4	Corning Microsheet Cover Glass After Dust Blasting 24 Hours, 50 km/hr., Diurnal Temperature Range. High Concentration of Pits in Border Area	26
4-5	Fused SiO_2 Cover Glass Prior to Blasting Was Smooth and Free of Imperfections	27
4-6	Fused SiO_2 Cover Glass After Dust Blasting 72 Hours, 100 km/hr., Diurnal Temperature Range. Approximately 40% of the Surface Is Pitted	27
4-7	Fused SiO_2 Cover Glass After Dust Blasting 72 Hours, 100 km/hr., Diurnal Temperature Range. Area of High Concentration of Overlapping Pits. About 10% of Original Surface Remains	28

ILLUSTRATIONS (Contd.)

4-8	Blasted SiO_2 Cover Glass. Details of Large Pits are Revealed at This High Magnification	28
4-9	Fused SiO_2. Linear Arrangements of Over-Lapping Pits	29
4-10	Unblasted Sapphire Cover Glass Appears Smooth and Clear at This Magnification	29
4-11	Sapphire Cover Glass After Dust Blasting 72 Hours, 100 km/hr., Ambient Temperature. The Surface Has a High Concentration of Very Small Pits	30
4-12	Integral Surface Covering. The Upper Half was Protected from the Dust Blast. Note the Imperfections. The Lower Half was Subjected to Dust Blasting 24 Hours, 50 km/hr., at Ambient Temperatures. Note the Dense Background of Fine Pits and Scattered Large Pits	30
4-13	Details of Pit Damage to Integral Surface Covering After Dust Blasting 72 Hours, 50 km/hr., at 245°K	31
4-14	Corning No. 0211 Microsheet. A network of Cracks Covered All Three Cover Glasses of This Assemblage After Dust Blasting 72 Hours, 50 km/hr., at Ambient Temperature. Oblique Illumination	31
4-15	Chipped Edge of Microsheet Cover Glass After Dust Blasting 72 Hours, 100 km/hr., Diurnal Temperature Range. Oblique Illumination	32
4-16	Orientation of Solar Cell Assemblage for Descriptive Purposes in Tables 4-1 Through 4-4	32

ILLUSTRATIONS (Contd.)

5-1	I-V Curves. Microsheet. Silver Mesh Connectors	52
5-2	I-V Curves. Microsheet. JPL Bus Bar Connectors	53
5-3	I-V Curves. Fused Silica. Silver Mesh Connectors	54
5-4	I-V Curves. Fused Silica. JPL Bus Bar Connectors	55
5-5	I-V Curves. Sapphire. Silver Mesh Connectors	56
5-6	I-V Curves. Sapphire. JPL Bus Bar Connectors	57
5-7	I-V Curves. Integral. Silver Mesh Connectors	58
5-8	I-V Curves. Integral. JPL Bus Bar Connectors	59
5-9	I-V Curves. Virgin Cells. Produced and Provided by JPL	60
5-10	I-V Curves. Cells after Testing and Cleaning. Produced and Provided by JPL	61

SECTION 1

INTRODUCTION

1.1 PURPOSE OF INVESTIGATION

Most items of equipment and scientific apparatus which are flown in space or landed on an extraterrestial body receive their power from solar cell assemblages. In space or on the lunar surface no environmental conditions have been encountered which have proved to be detrimental to the operation of solar cell assemblages. On the surface of Mars, however, the observed and postulated environmental conditions are unlike those in space and on the surface of the Moon. The presence of an atmosphere on Mars, extremely thin though it may be, produces an environment which may include phenomena which will effect the performance of solar cells. Equipment and apparatus may become inoperative as a result.

The one postulated phenomenon which may seriously reduce the efficiency of solar cells in the Martian environment is the dust storm. Yellow cloud-like features usually observed in the equatorial regions have been interpreted as dust storms (Maginni, 1939; de Vaucouleurs, 1954; Dolphus, 1961; Slipher, 1962). These "clouds" have linear dimensions which range from 400 to 2000 km. The velocity of movement of the

clouds varies over a considerable range with an average estimated to be about 40 km/hr. Speeds as high as 135 km/hr have been observed (Gifford, 1964). The lower limit of frequency of the storms is approximately one per year and the duration ranges from one day to over three days.

It is necessary to determine the effects of dust storms on solar cell performance under various environmental conditions that can be expected on Mars. In order to accomplish this a program of experiments was devised in which solar cell assemblages were subjected to blowing dust under specified environmental conditions for specified periods of time. Changes in performance of solar cells were determined and damage to assemblages and cover glasses assessed and analyzed.

SECTION 2

CONDITIONS AND DESIGN OF EXPERIMENTS

2.1 SIMULATED MARTIAN ENVIRONMENT

Data concerning the environmental conditions on Mars are summarized and analyzed in Mars Scientific Model, JPL Document No. 606-1, July 15, 1968, and from these data were chosed certain values for wind velocities, temperatures and temperature ranges, and for the composition of the atmosphere. The chosen values were approved by JPL. It was agreed that tests were to be conducted under the following conditions:

Temperatures:	(a) ambient (290°-300°K)
	(b) 245°K
	(c) diurnal range 210°-305°K
Wind velocities:	(a) 50 km/hr
	(b) 100 km/hr
Atmosphere:	CO_2 plus trace of water. (amount of H_2O vapor was 0.01 $\pm$ 0.005% by volume)

No provision for simulation of the atmospheric surface pressure on Mars was made.

2.2 PARTICULATE MATTER

Data gathered by means of remote sensing devices concerning

the surface material of Mars is not conclusive. If we assume that the terrestrial planets and the Moon originated at about the same time and as a result of the same processes, their compositions should be similar. Alteration of the minerals of which rocks are composed occurs at and immediately below the surface of the Earth as a result of weathering processes. This is because of the Earth's atmospheric envelope which contains active substances principally oxygen, carbon dioxide and water vapor. The resulting particulate matter available for transportation by wind is mostly quartz and secondary minerals, principally clay minerals. This sand and dust would be quite different from what would accumulate on the Martian surface. There in the presence of the rarified atmosphere composed principally of CO_2 and possibly a trace of water vapor a minimum of chemical alteration should occur. Various investigators (Adams, 1968, Binder and Cruikshank, 1964, Loomis, 1967, O'Leary, 1967, Sinton, 1967, and Younkin, 1966) have postulated that the particles are coated with ferric oxides, sub-hydrates and possibly ferrous carbonates. For the most part the particles should be fine pyroclastic ejecta and particles formed by meteor impact.

With the exceptions of minor weathering products the Martian surface sand and dust should be similar to that on the Moon.

It was agreed that the particulate matter to be used in the simulated Martian dust storms should resemble as closely as possible the fine material in the lunar soil samples obtained by the astronauts of Apollo 11. Olivine basalt which was collected in the Hudson Mountains, Ellsworth Land, Antarctica, was used. The principal constituents are clinopyroxene, plagioclase and olivine. A small amount of glass is present. This differs somewhat from the lunar fines which run about 50% glass and contain considerable ilmenite in addition to the essential minerals in the Antarctic rock. It is believed that these compositional differences did not alter the results of the tests significantly. The fines in the lunar soil material from the "bulk box" ranges considerably in size. However, approximately 45% were in the 125-62.5 micron range and 25% in the less than 62.5 micron range.

Wind tunnel tests have shown that movement of particles of less than 60 microns in size will not be initiated by wind velocities of 100 km/hr or less. The presence of slightly larger particles is necessary to initiate movement. Larger particles move by the process of saltation and with every bounce finer particles are knocked into the air stream where they remain in suspension, buoyed up by the turbulent air.

Based upon observations of dust storms in the tunnel, it was decided that 'worst case' conditions could be obtained by using a mixture of particulate matter of 75% in the 125-250 micron range and 25% in the <62.5 micron range. These are weight percentages.

2 3 DESCRIPTIONS OF WIND TUNNELS

The wind tunnel for test experiments at ambient temperatures and preliminary tests was constructed mainly of quarter inch plexiglass. It is essentially a closed system shaped like a race track, Figure 2.1. The "atmosphere" is circulated with a squirrel cage blower which is driven by a heavy duty electric motor. Wind velocities in the straight-away sections of the race track where the solar cell assemblages are placed during tests are controlled by varying the cross section.

Two pairs of straight-away sections were used. With one pair a wind velocity of 50 km/hr is maintained; with the second 100 km/hr. With this arrangement no variations in blower rpm are necessary to produce the desired velocities. Solar cell assemblages to be tested are mounted on weighted brackets in such a way that the entire outer face of each cell and the wire connectors are exposed to the dust storms.

Before assembling the wind tunnel an adequate amount of 'Martian dust' is distributed in the various sections. Prior to each test the atmosphere in the tunnel is swept out and replaced with CO_2 gas in which there is a trace of water vapor. The commercial CO_2 gas which was used contained $0.01 \pm 0.005\%$ water vapor by volume. As the entire system was sealed before each test no water vapor could enter from the outside during a test. The reason for the use of plexiglass in the construction of the tunnel is to make possible direct view of the dust storms. During preliminary tests it was noted that there was considerable turbulence in the curved sections of the tunnel, but that the flow in the straight sections was essentially laminar. When the assemblages containing the solar cell modules are introduced in the system, local turbulence is developed because of their presence in the air current.

For those tests which required temperature control a second tunnel was constructed. The basic design was similar to that of Tunnel No. 1. The curved and connector sections, however, were constructed of 1/4" sheet metal; only the straight sections in which the solar assemblages were positioned were made of plexiglass. The entire tunnel was then sealed in a casing of 1" sheet styrofoam to insulate

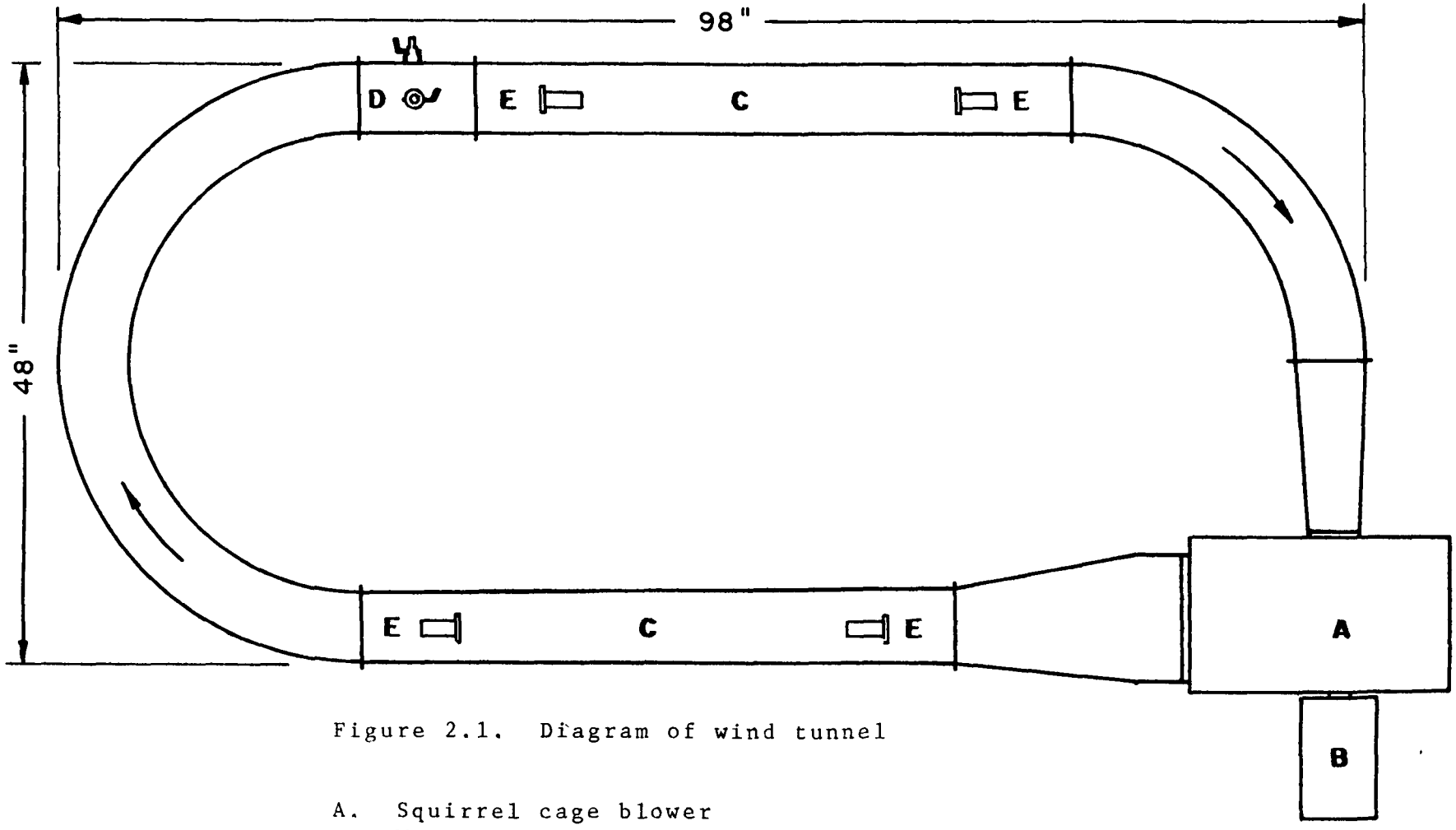

Figure 2.1. Diagram of wind tunnel

A. Squirrel cage blower
B. Motor
C. Removable straight-away sections
D. Valve section. CO_2 inlet and outlet
E. Solar cell assemblages

it. There was sufficient spacing between the top of the tunnel sections and the styrofoam to permit the introduction of slabs of solid CO_2, two inches thick. Provision was made for the introduction or removal of blocks of CO_2 from the tops of the metal portions of the tunnel in order to control the temperature of the atmosphere within. Through experimentation it was learned that by maintaining a certain amount of solic CO_2 in the system the temperature could be lowered to 245°K $\pm$ 5° and be maintained there indefinitely. Also, by introductions of solid CO_2 blocks and their partial or complete removal at specified times a diurnal variation closely approximating the specified limits, 210°K - 305°K, was produced. These tests were run during summer when room temperatures exceeded 305°K. Temperature was taken at intervals of one or two hours.

2.4 SOLAR CELL ASSEMBLAGES AND SOLAR CELL COVER GLASSES

JPL provided 96 solar cell assemblages and additional cover glasses for use in the project. Each assemblage was composed of three "N/P type" solar cells each of which measures 2 cm x 2 cm x .035 cm. Contacts were titanium-silver, centered. Cells were coated with silicon monoxide anti-reflecting to peak transmission of 0.5 - 0.8 microns. Cover glass adhesive was RTV-602. The integral cells were of the

borosilico fused glass type. Base resistivity of cells tested ranged from 7 to 14 ohm-centimeters.

Each of two sets of 48 assemblages contained the following:

12 with Corning No. 0211 microsheet cover glasses
12 with fused SiO_2 cover glasses
12 with sapphire cover glass
12 of the integral type

The sets differed only in the type of electrical interconnections. In one a silver mesh was used and in the second the JPL Bus Bar. With two sets repeat runs could be programmed and the comparative reliability of the two types of interconnections determined.

In each test four assemblages were to be exposed to dust storms under certain environmental conditions as shown in Figure 2-2. As each of the four assemblages had a different covering material, their relative resistance to damage due to impact by particulate matter could be determined.

2.5 EXPERIMENTAL PROGRAM

Each solar cell assemblage was examined under the microscope at magnifications of 10 and 20 and all imperfections on each cover glass were recorded. A current-voltage curve was then made for each assemblage (See Section 5 for details of the procedure). Four assemblages, each with a different type

cover glass, were then placed in the wind tunnel and subjected to a dust storm under certain environmental conditions for a specified period of time. At the conclusion of the test period in the wind tunnel a second current-voltage curve was made for each assemblage.

Because a coating of dust accumulated on all solar cell cover surfaces during dust storms, it was necessary to remove the dust and then make a third current-voltage curve for each assemblage. From the three curves it was possible to determine what part of the reduction in efficiency of the solar cells was due to the dust coating and what portion to permanent damage to the covering materials. After the cells had been cleaned they were again subjected to microscopic examinations at various magnifications and all damage assessed and recorded.

The program of testing is summarized in Figure 2-2.

Days	Vel. Km/Hr	Atmos. CO_2 + trace H_2O	TEMPERATURES: AMBIENT — SOLAR CELL PROTECTION: Corning #0211 Microsheet A	Corning #0211 Microsheet B	Quartz A	Quartz B	Sapphire A	Sapphire B	Integral Glass Covers A	Integral Glass Covers B
1	50	X	X	X	X	X	X	X	X	X
	100	X	X	(X)	X	(X)	X	(X)	X	(X)
3	50	X	X	X	X	X	X	X	X	X
	100	X	X	X	X	X	X	X	X	X

Days	Vel. Km/Hr	Atmos. CO_2 + trace H_2O	TEMPERATURES: AVERAGE (245°K) — SOLAR CELL PROTECTION: Corning #0211 Microsheet A	Corning #0211 Microsheet B	Quartz A	Quartz B	Sapphire A	Sapphire B	Integral Glass Covers A	Integral Glass Covers B
1	50	X	X	(X)	X	(X)	X	(X)	X	(X)
	100	X	X	X	X	X	X	X	X	X
3	50	X	X	X	X	X	X	X	X	X
	100	X	X	X	X	X	X	X	X	X

Days	Vel. Km/Hr	Atmos. CO_2 + trace H_2O	TEMPERATURES: DIURNAL CYCLE (210°K to 305°K) — SOLAR CELL PROTECTION: Corning #0211 Microsheet A	Corning #0211 Microsheet B	Quartz A	Quartz B	Sapphire A	Sapphire B	Integral Glass Covers A	Integral Glass Covers B
1	50	X	X	X	X	X	X	X	X	X
	100	X	X	X	X	X	X	X	X	X
3	50	X	X	X	X	X	X	X	X	X
	100	X	X	X	X	X	X	X	X	X

A = Expanded silver mesh

B = JPL bus bar Dwg #10016709-1

Figure 2-2. Program of testing. With the exceptions of those circled, the tests were completed. One assemblage was placed at each of the test points.

SECTION 3

DUST COATINGS ON SOLAR CELLS

3.1 DEVELOPMENT OF DUST COATINGS

During the tests conducted at ambient temperatures when the interior of the tunnel could be viewed, it was noted that a coating of dust collected on the solar cell assemblages as soon as the dust storm started. Whether or not this coating continued to build during the entire dust storm period could not be determined. Some abrasion of the coating might have occurred also.

3.2 DESCRIPTION OF DUST COATINGS

All solar cell assemblages when removed from the wind tunnel after a test were coated with dust (See Figures 3-1 and 3-2 for appearances before and after test). The coatings were not uniform in thickness. Some were quite thin and the wires of the solar cells were visible through them, Figure 3-2. In other cases the coatings might be as much as 0.5 mm thick and opaque.

Some coatings seemed to be loose aggregates of dust particles, others had the characteristics of cement. The type of coating varied from test to test but was the same on the four assemblages subjected to the same test (Figure 3-3).

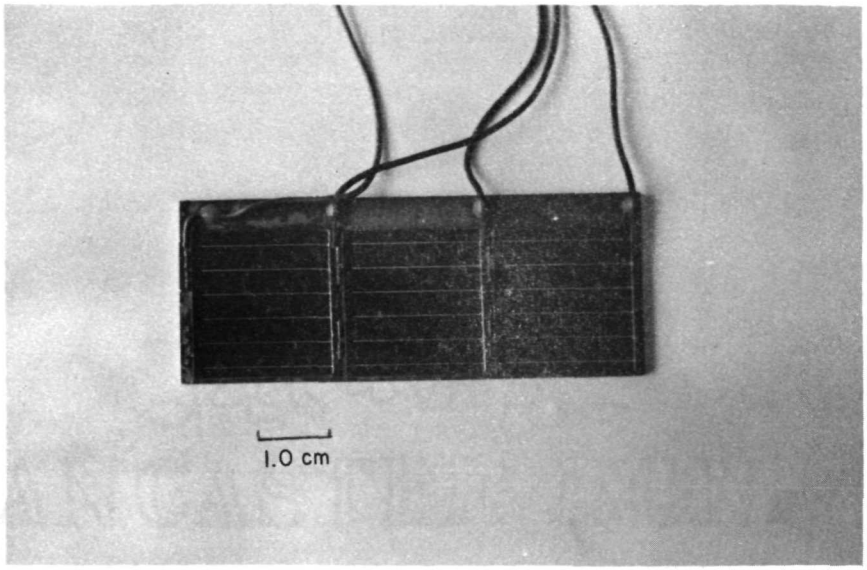

Figure 3-1. Solar cell assemblage before dust blasting

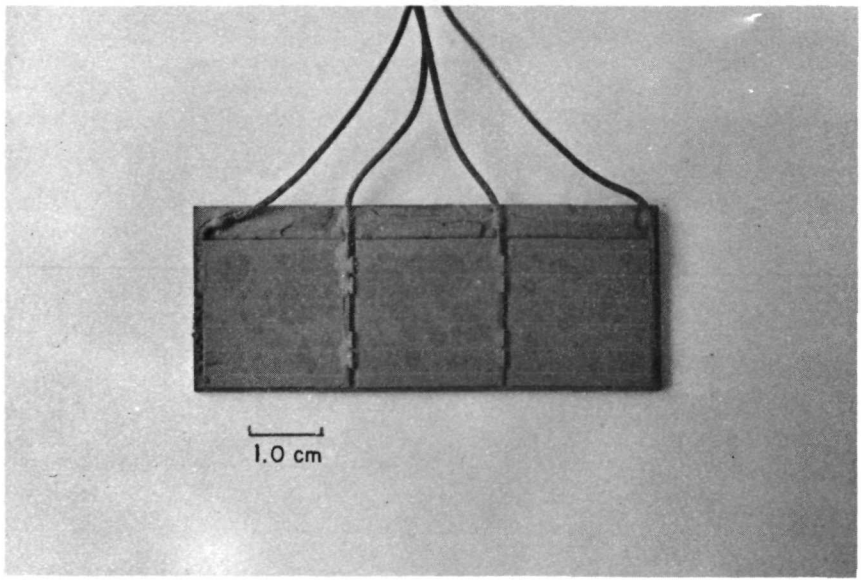

Figure 3-2. Solar cell assemblage with thin layer of dust which was deposited during "dust storm" of 24 hours, 100 km/hr., ambient temperature

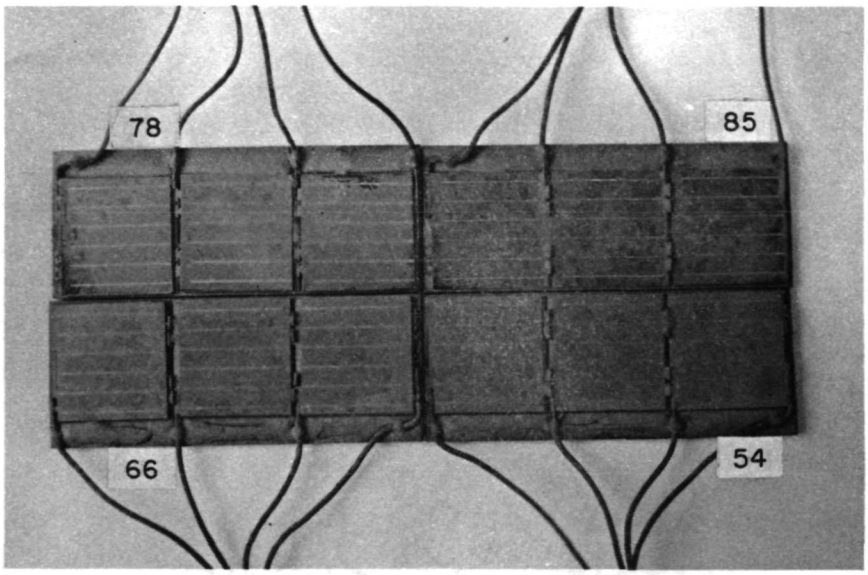

Figure 3-3. Four solar cell assemblages which had been subjected to same dust storm. Note simularities of dust coatings

No. 54 - Corning microsheet
No. 66 - Fused SiO_2
No. 78 - Sapphire
No. 85 - Integral

No direct correlation between type of coating and environment was noted. The hard, thick coatings, however, developed most frequently when the test temperatures were held at 245°K or varied over the diurnal range.

It was suspected that variations in the water content of the test atmospheres might be responsible for variations in coatings. Some leakage of the atmosphere of the room in which the wind tunnels were housed into the system might have occurred. Since the joints were well sealed, however, this seems unlikely.

3.3 REMOVAL OF DUST COATINGS

Differences in the characteristics of the coatings became obvious when cleaning of the cover glasses was attempted. In a few cases a blast of compressed air would remove most of the dust and the remainder was easily washed off in water. Final cleaning was accomplished by use of cottom swabs saturated with"Windex" followed by dry swabbing. This last operation was performed while viewing through a binocular microscope at 10 or 20 magnifications.

The hard cakes of dust were removed with great difficulty. A stream of compressed air had no effect. They were not loosened by soaking in water or "Windex". In many cases it

was necessary to pry them loose with a thin-edged scalpel. This operation had to be performed with extreme care in order to prevent additional damage to the cover glasses. These cakes adhered tightly to the basal plate where exposed, to the exposed portion of the connecting wires, and the edges of the cells, as well as to the cover glasses.

SECTION 4

PERMANENT DAMAGE TO SOLAR CELLS AND COVER GLASSES

4.1 SUMMARY

The permanent damage to the solar cell assemblages sustained during dust storms was considerable. All four types of cover glasses were damaged in one or more ways and in all of the test environments. Damage is placed in four categories: (1) pitting of cover glass surface due to impact of wind driven particles, (2) cracking and chipping of cover glasses, (3) unbonding of cover glasses, and (4) failure of electrical interconnections.

Greatest damage due to pitting was sustained by the fused SiO_2 cover glasses, then in descending order of magnitude, Corning No. 0211 microsheet, integral and sapphire. Cracking and chipping of the cover glasses was considerable in the case of Corning No. 0211 microsheet, particularly those subjected to low temperatures. 56.1% of the microsheet cover glasses were cracked to some extent. 22.7% of the sapphire cover glasses were cracked to a minor degree.

Cracking was unimportant in the cases of fused SiO_2 and integral cover glasses. The variation in the resistance to cracking by the three cover glass materials is probably related to their respective lattice energies. Because of the thickness of the integral material, no cracking would be probable.

The unbonding of cover glasses is a serious matter in the cases of the sapphire and microsheet types. Forty-two of 66 sapphire cover glasses became partially or completely loosened. Twelve of 66 microsheet glasses became partially or totally unbonded. Bonding is successful when the cementing material penetrates the surfaces of the materials to be bonded. Penetration of the cement is controlled by the spatial arrangement of the ions, atoms, partial molecules, etc. in the cover glass materials. It appears from the results that the penetration of the bonding cement was adequate in the case of the fused SiO_2 only.

Only one electrical interconnection failed during the testing operations. It was of the silver mesh type.

4.2 PITTING OF SURFACES BY WIND-DRIVEN PARTICLES

Surfaces of all types of cover glasses were damaged by impact of wind-driven rock particles in the two size

ranges, <60 and 125-250 microns diameters. The amount and character of the damage varied from practically nil to very great. The amount and character of impact damage was controlled by the distribution of the dust cover on each cover glass and the rapidity of accumulation of the dust cover. Coatings were not uniform because of local turbulences in the air currents. Distribution and thickness of coating varied from cover glass to cover glass and from experiment to experiment. Significant differences in the amount and character of the damage to each of the four different surfaces was, however, obvious. A summary of pit damage to each type is presented.

4.2.1 CORNING NO. 0211 MICROSHEET

Surfaces of the microsheet cover glasses were examined microscopically before subjecting them to dust storms and found to be smooth, clear and with only a few imperfections, Figure 4-1. After subjection to dust storms of velocities of either 50 or 100 km/hr., the surfaces exhibited a general background of extremely small pits and a scattering of larger pits, Figures 4-2 and 4-3. Higher concentrations of the larger pits were present in the areas which had not been well protected by dust coatings, usually in marginal or corner areas, Figure 4-4.

No significant differences in the degree of damage under different environmental conditions were noted.

4.2.2 FUSED SiO_2

The unblasted cover glasses were smooth and clear with few imperfections, Figure 4-5. Because of the dust cover which accumulated on the cover glasses during blasting, no damage was discernable until after cleaning. When clean the damage due to pitting was easily noted, even with the unaided eye. Pits of many sizes were present, but three size ranges dominate the assemblage of pits, Figure 4-6. In some areas pits were so numerous that less than 10% of the original surface remained, Figure 4-7. Under high magnification, 320X, details of the pits are discernable, Figure 4-8. The resemblance to the surface of a pahoehoe lava flow is striking and it is tentatively concluded that plastic flow with a minimum of shattering took place. Another interesting observation is the occasional linear arrangement of pits with the lines producing geometric patterns, Figure 4-9. This may reflect the partially disordered arrangement of the Si and O atoms in the fused SiO_2 space lattice.

4.2.3 SAPPHIRE

The sapphire cover glasses were clear, smooth, and with

no surface imperfections prior to subjection to simulated dust storms, Figure 4-10. Of the 22 assemblages with sapphire cover glasses that were tested in the wind tunnels, 19 exhibited pitting. Pits were very small and in most cases concentrated in borders or corners, Figure 4-11. Central areas of some cover glasses remained undamaged.

4.2.4 INTEGRAL

The so-called integral type covering exhibited many pit-like imperfections prior to dust blasting. Also the surfaces had a rough appearance when observed under the microscope at 50 or higher magnifications, Figure 4-12. These original features made assessment of damage due to dust storms extremely difficult. That damage did result, however, is evident in Figure 4-12. A portion of the cover glass was protected by a clamp during the "dust storm" thus preserving some of the original surface for comparative purposes. Bombardment with dust particles increased the roughness of the surface in general and resulted in true pitting, Figures 4-12 and 4-13. The integral covers on 15 of the 22 assemblages subjected to "dust storms" were damaged.

4.3 CRACKING AND CHIPPING OF COVER GLASSES

Two of the four types of cover glasses were damaged

severely by cracking and one by chipping along the edges. The Corning No. 0211 microsheet exhibited the greatest amount of cracking and chipping. Sapphire cover glasses were damaged by cracking to a lesser extent. Only one fused SiO_2 cover glass was cracked and, because of its construction, the integral covers escaped this type of damage.

4.3.1 CORNING NO. 0211 MICROSHEET

Thirty-seven of the 66 microsheets tested in the wind tunnels were cracked during the dust blasting. The type and amount of cracking varied considerably from single short cracks to a network of cracks segmenting an entire cover glass, Figure 4-14. Chipping of edges was a common phenomenon, Figure 4-15. Some cracks originated at the edge of a cover glass, others in the central areas. Crack damage to each cover glass is presented in Table 4-1. Although the evidence is not conclusive, it appears that the microsheet cover glasses crack more readily when subjected to low temperatures or diurnal temperature ranges of 95°K.

4.3.2 SAPPHIRE

Sixteen of the 66 sapphire cover glasses were cracked during "dust storms". Many cracks were short, that is,

one to five mm long. Some originated at edges, others in the central areas. No chipping of the edges was noted. Crack damage to each cover glass is presented in Table 4-2. The evidence appears to indicate that the sapphire cover glasses may be somewhat more vulnerable to this type of damage when subjected to a wide range of temperatures.

4.3.3 FUSED SiO_2

Only one fused SiO_2 cover glass cracked during the test operations. Chipped edges developed on three cover glasses of this type.

4.4 UNBONDING OF COVER GLASSES

It became apparent during the testing operations that the type of material, RTV-602, used to secure the cover glasses to the solar cells was not adequate for the task. Partial or complete unbonding of twelve of 66 microsheet cover glasses occurred and 42 of 66 of the sapphire type. No unbonding of the fused SiO_2 cover glasses was noted. The details of unbonding of the microsheet cover glasses are presented in Table 4-3 and for sapphire cover glasses in Table 4-4.

Twenty-one microsheet cover glasses were tested at ambient temperatures, failure of bonding occurred in two cases.

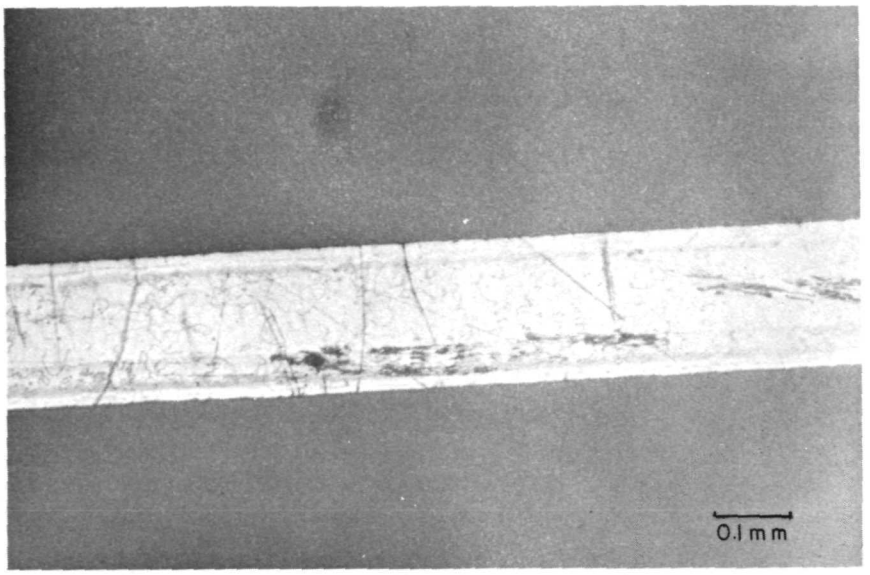

Figure 4-1. The Corning No. 0211 microsheet cover glasses were free of surface imperfections before subjecting them to dust storms

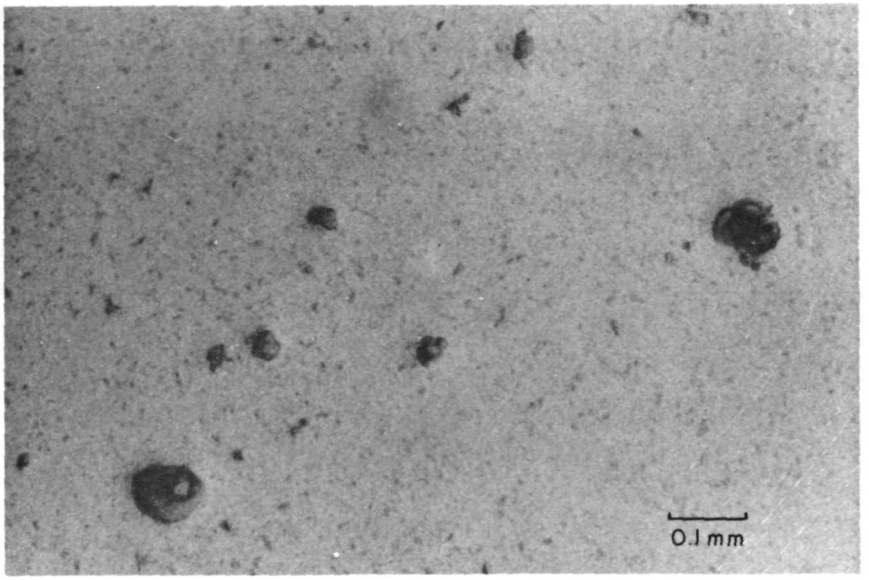

Figure 4-2. Corning microsheet cover glass after dust blasting 24 hours, 50 km/hr., 245°K. Note the background of fine pits and the scattered medium- and large-size pits

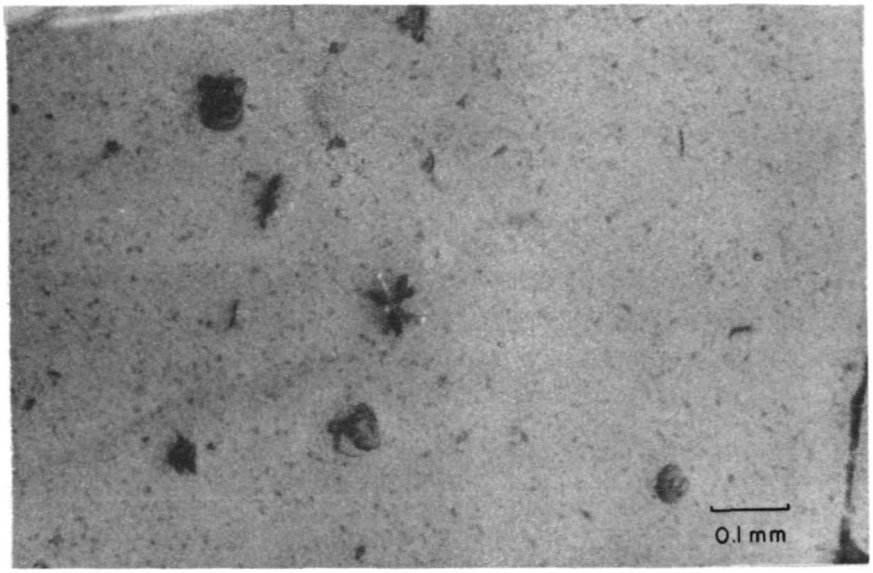

Figure 4-3. Same as Figure 4-2, but of different area. Note crater-like pits and one radiating-type pit

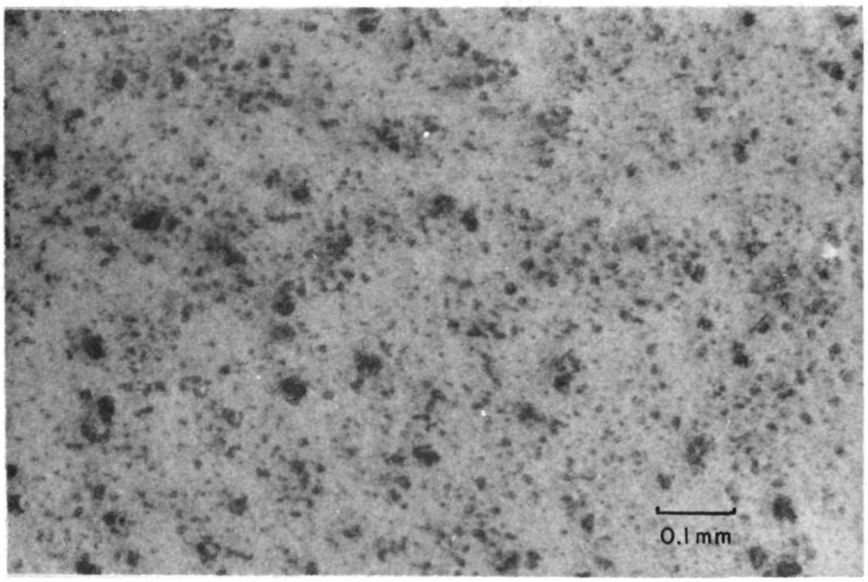

Figure 4-4. Corning microsheet cover glass after dust blasting 24 hours, 50 km/hr., diurnal temperature range. High concentration of pits in border area

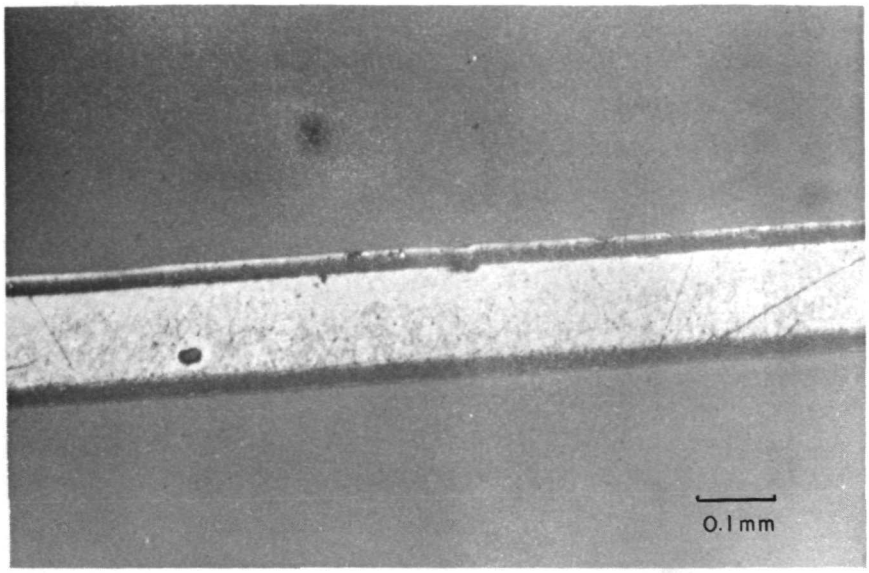

Figure 4-5. Fused SiO_2 cover glass prior to blasting was smooth and free of imperfections

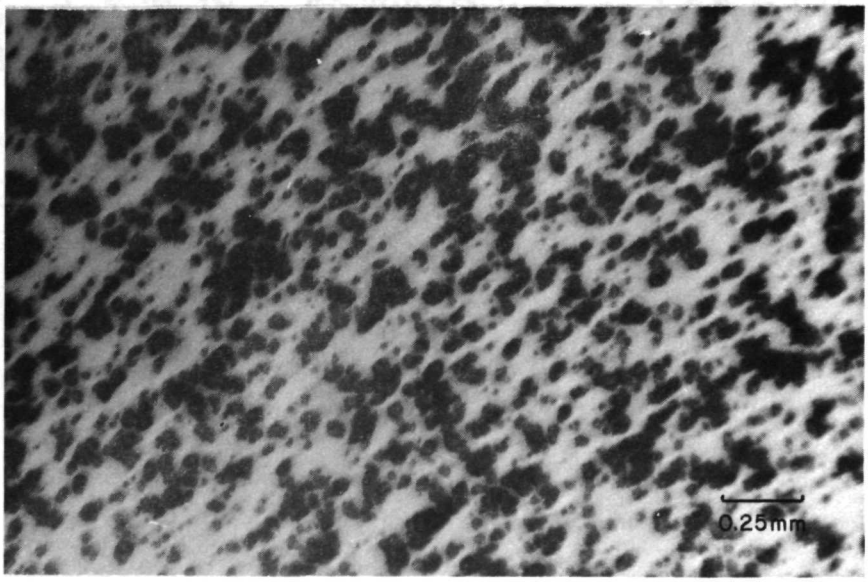

Figure 4-6. Fused SiO_2 cover glass after dust blasting 72 hours, 100 km/hr., diurnal temperature range. Approximately 40% of the surface is pitted

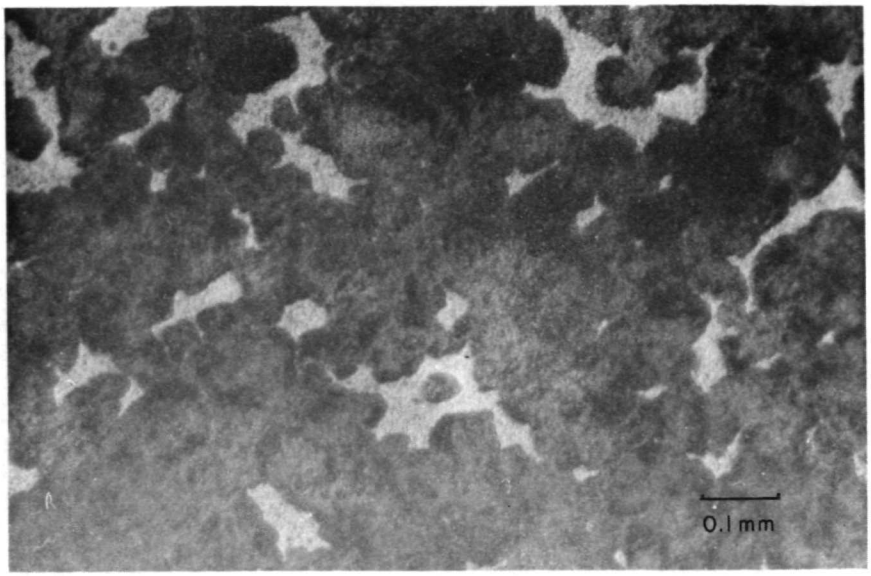

Figure 4-7. Fused SiO_2 cover glass after dust blasting 72 hours, 100 km/hr., diurnal temperature range. Area of high concentration of overlapping pits. About 10% of original surface remains

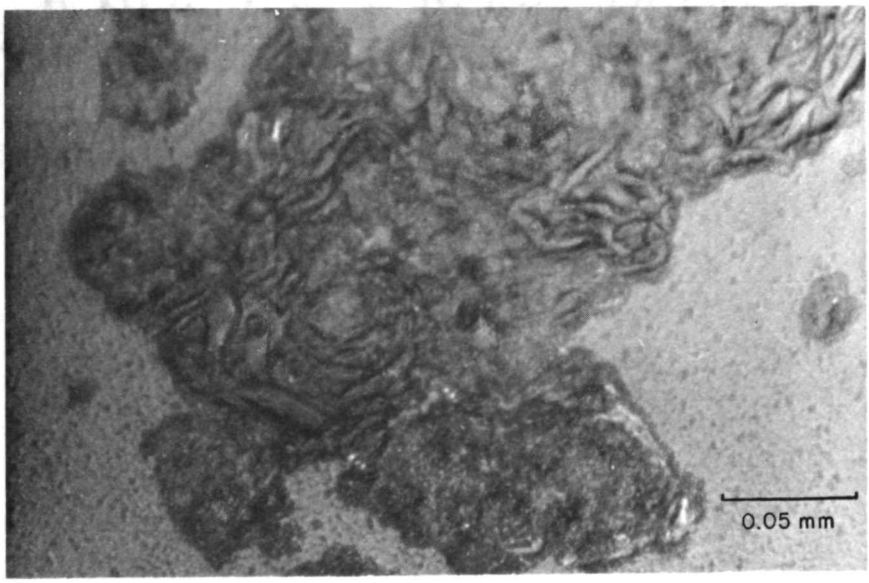

Figure 4-8. Blasted SiO_2 cover glass. Details of large pits are revealed at this high magnification

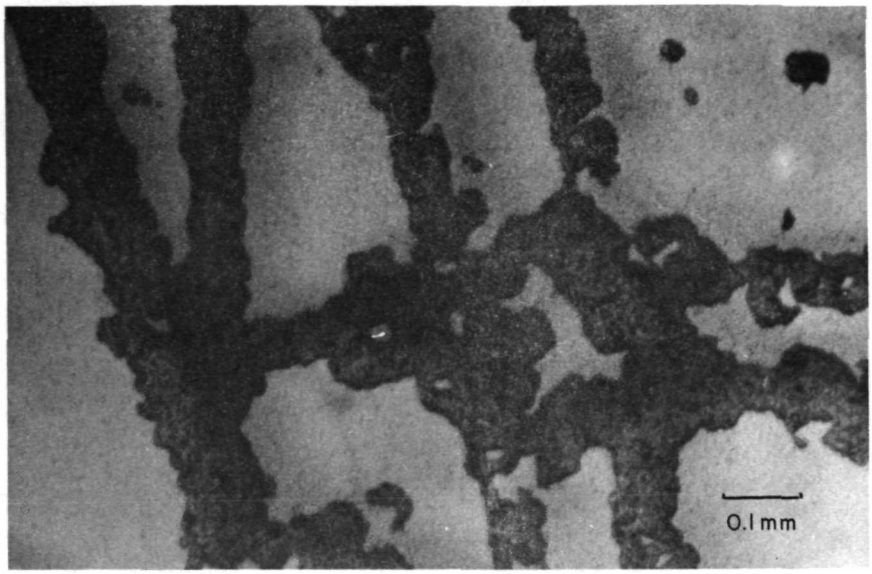

Figure 4-9. Fused SiO_2. Linear arrangements of overlapping pits

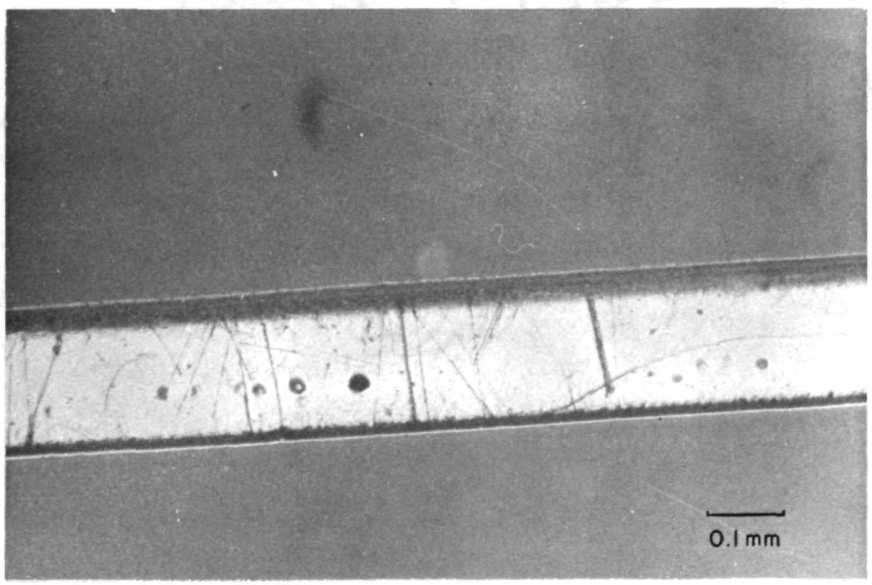

Figure 4-10. Unblasted sapphire cover glass appears smooth and clear at this magnification

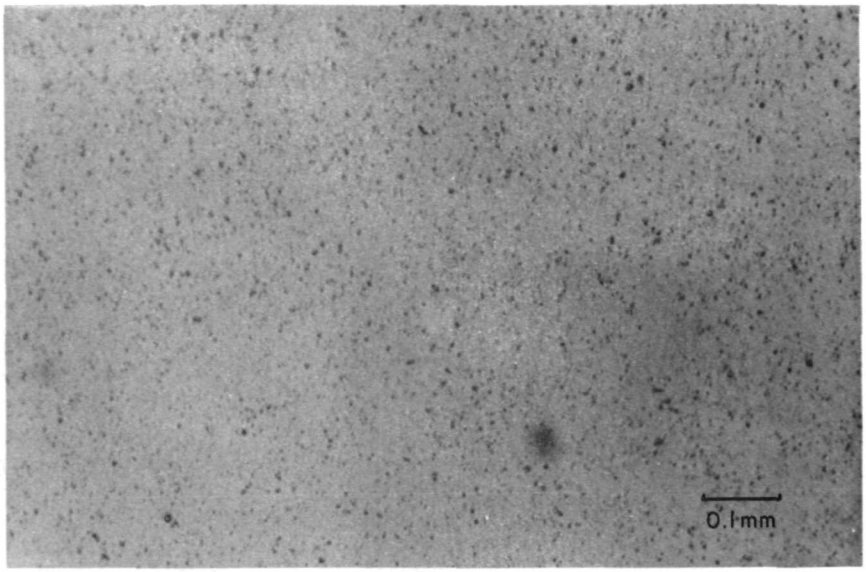

Figure 4-11. Sapphire cover glass after dust blasting 72 hours, 100 km/hr., ambient temperature. The surface has a high concentration of very small pits

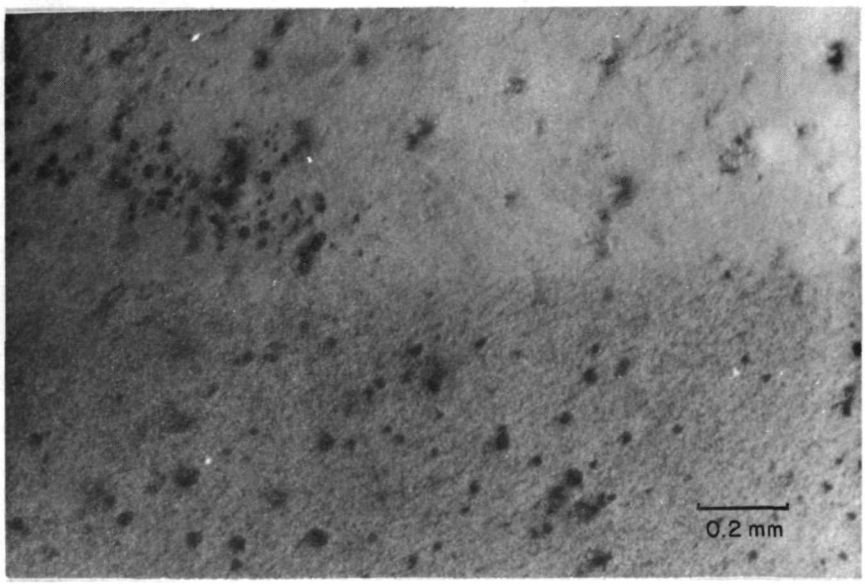

Figure 4-12. Integral surface covering. The upper half was protected from the dust blast. Note the imperfections. The lower half was subjected to dust blasting 24 hours, 50 km/hr., at ambient temperatures. Note the dense background of fine pits and scattered large pits

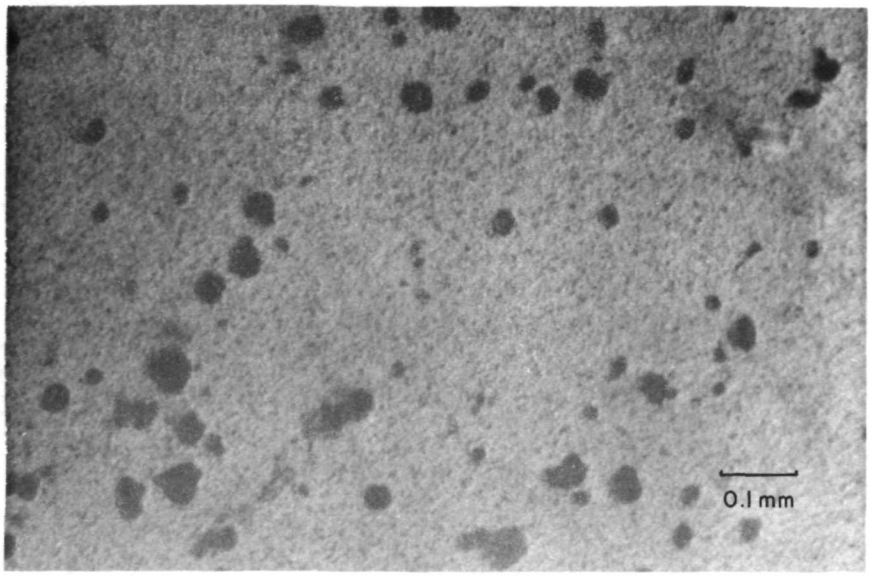

Figure 4-13. Details of pit damage to integral surface covering after dust blasting 72 hours, 50 km/hr., at 245°K

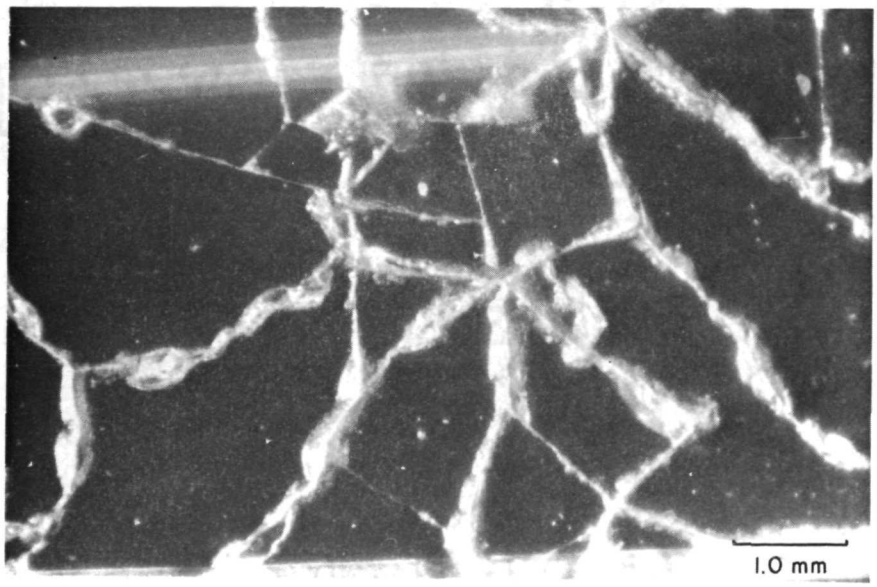

Figure 4-14. Corning No. 0211 microsheet. A network of cracks covered all three cover glasses of this assemblage after dust blasting 72 hours, 50 km/hr., at ambient temperature. Oblique illumination

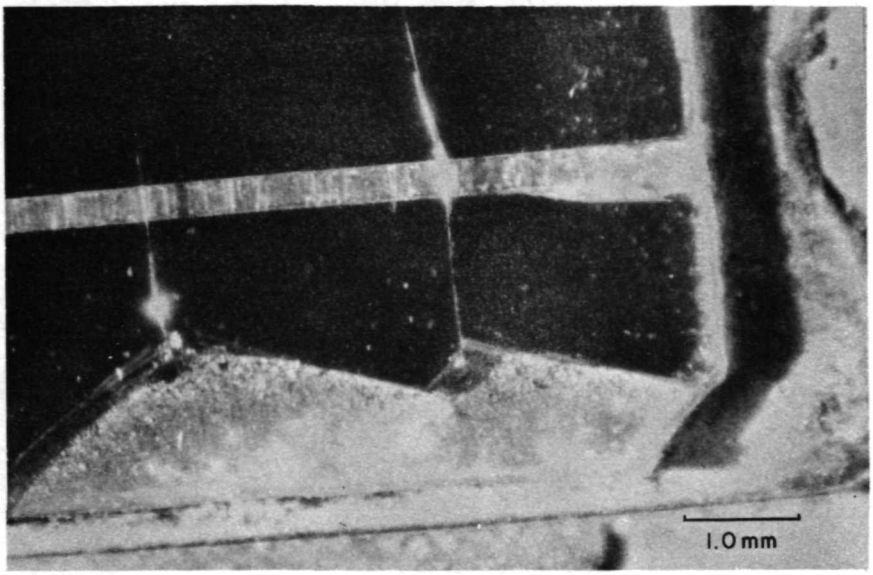

Figure 4-15. Chipped edge of microsheet cover glass after dust balsting 72 hours, 100 km/hr., diurnal temperature range. Oblique illumination

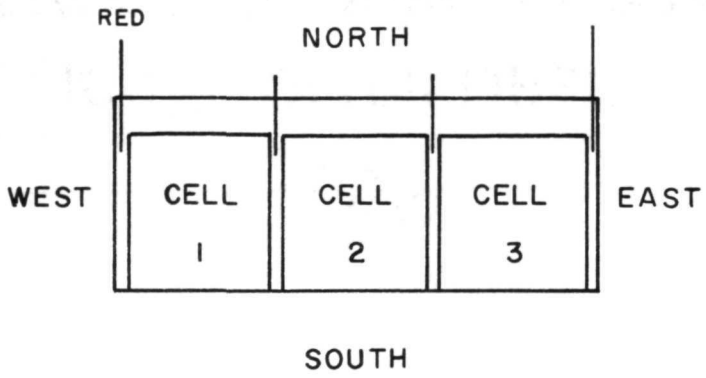

Figure 4-16. Orientation of solar cell assemblage for descriptive purposes in Tables 4-1 through 4-4

Twenty-one were tested at 245°K, five of these cover glasses became partially or completely unbonded. Five of the 24 microsheet cover glasses tested in a diurnal temperature range of 95°K became partially or completely unbonded.

With sapphire cover glasses failure of bonding occurred as follows: at ambient temperatures, six of 21; at 245°K, 15 of 21; with diurnal variation, 21 of 24.

4.5 FAILURE OF ELECTRICAL INTERCONNECTIONS

No significant damage to the electrical interconnections on the solar cell assemblages occurred during the testing procedures. One wire became disconnected on assemblage No. 14 during a dust storm of 72 hours duration, 50 km. per hour, ambient temperatures. This interconnector was of the silver mesh type.

4.6 ANALYSIS OF DAMAGE DATA

From the data in Table 4-5 it is indicated that temperature is an important factor in the overall process which results in cracking of microsheet during wind tunnel tests. Greatest crack damage occurred during tests in which the temperature was held at 245°K., somewhat less during the tests in which the temperature ranged from 210°K to 305°K in a period of 24 hours, and least when tunnel temperature

was ambient. Significant increase in damage occurred when the time interval was increased from 24 hours to 72 hours at ambient temperature and at 245°K. On the other hand a decrease in crack damage is noted in the case of diurnal temperature range from a one day period to one of three days. Wind velocity appears to play an insignificant role in the overall process.

Analysis of data in Table 4-6 does not reveal any significant differences in the amounts of crack damage sustained by sapphire cover glasses in the different test environments. Perhaps the most noteworthy is the small increases at low and ranging temperatures.

Unbonding of microsheet cover glasses is significantly greater at 245°K than at ambient temperatures. Variation in temperature during test periods appears to play an insignificant role in the process. See Table 4-7. Of no significance are the difference in amounts of unbonding during the 24-hour and 72-hour test periods, nor with the variations in wind velocity.

That the material, RTV-602, used to bond the sapphire cover glasses to the solar cells did not do so satisfactorily is obvious from the data analyzed in Table 4-8. There was 63.5% partial or complete failure. Failure of

45.7% at ambient temperatures indicates that the adhesive was not bonding with the sapphire as it did with fused SiO_2 with which there were no failures. Increase in bonding failures at 245°K and over the diurnal range is significant. These data suggest that there is a significant difference in the coefficients of expansion of the adhesive and the sapphire cover glasses. Differential expansion and contraction of the two materials results in weakening of an already poor bond.

No pattern could be derived concerning the amounts of damage by pitting in the several environments.

4.7 CONCLUSIONS

All types of cover glasses used in the tests were damaged in one or more ways during simulated Martian dust storms. The Corning No. 0211 microsheet was severely damaged by cracking and chipping and to a moderate degree by pitting. The fused SiO_2 cover glasses were severely pitted. Major damage to sapphire cover glasses was by cracking, but to a lesser degree than that developed in the microsheets.

Sapphire resisted pitting better than the other three types. The integral covering material was damaged by pitting to a moderate degree. Unbonding of sapphire and

microsheet cover glasses is a critical matter, but one that can be resolved. A variety of bonding materials is available. A series of tests should be run to determine which is most satisfactory with sapphire and which with microsheet. The tests should include low temperature as well as ambient temperature environments.

Both the silver mesh and JPL Bus Bar types of electrical interconnections in the solar cell assemblages withstood the dust storms equally well. The one failure was probably because of a poor soldering job.

It is the opinion of the principal investigator that none of the four types of cell covering materials is satisfactory for protection against dust and sand blasting. The least objectionable would be the integral and in order of decreasing desirability would be sapphire, microsheet, and fused SiO_2.

TABLE 4-1

DAMAGE TO SOLAR CELL COVER GLASSES

Cracks

CORNING No. 0211 Microsheet

Assemblage No.	Environment	Cell No.	Damage
1	24hr/100km/ diurnal	1 2 3	network of cracks over 35% of surface scattered cracks few cracks
2	24hr/50km/ambient	1 2 3	few cracks few cracks no cracks
3	72hr/50km/ambient	1 2 3	no cracks no cracks no cracks
4	24hr/100km/ambient	1 2 3	no cracks no cracks no cracks
5	72hr/100km/ambient	1 2 3	few cracks few cracks no cracks
6	24hr/50km/245°K	1 2 3	many cracks many cracks many cracks

TABLE 4-1

DAMAGE TO SOLAR CELL COVER GLASSES

Cracks

CORNING No. 0211 Microsheet

Assemblage No.	Environment	Cell No.	Damage
7	72hr/50km/diurnal	1 2 3	no cracks no cracks one major crack
8	72hr/100km/245°K	1 2 3	one small crack few cracks few cracks
9	72hr/50km/245°K	1 2 3	one crack few cracks few cracks
10	24hr/50km/diurnal	1 2 3	few cracks one major and few small cracks few cracks
11	24hr/100km/245°K	1 2 3	one major and few small cracks no cracks no cracks
12	72hr/100km/diurnal	1 2 3	few cracks major crack major crack

TABLE 4-1

DAMAGE TO SOLAR CELL COVER GLASSES

Cracks

CORNING No. 0211 Microsheet

Assemblage No.	Environment	Cell No.	Damage
49	not used		
50	24hr/50km/ambient	1 2 3	no cracks no cracks no cracks
51	72hr/100km/ambient	1 2 3	one major crack no cracks no cracks
52	72hr/50km/ambient	1 2 3	network of cracks over entire surface network of cracks over entire surface network of cracks over entire surface
53	72hr/100km/diurnal	1 2 3	one crack no cracks no cracks
54	not used		

TABLE 4-1

DAMAGE TO SOLAR CELL COVER GLASSES

Cracks

CORNING No. 0211 Microsheet

Assemblage No.	Environment	Cell No.	Damage
55	72hr/50km/245°K	1 2 3	few cracks few cracks no cracks
56	24hr/50km/diurnal	1 2 3	one major and few small cracks no cracks no cracks
57	72hr/50km/diurnal	1 2 3	no cracks no cracks network of cracks over 20% of surface
58	24hr/100km/245°K	1 2 3	no cracks minor crack no cracks
59	24hr/100km/diurnal	1 2 3	two small cracks no cracks no cracks
60	72hr/100km/245°K	1 2 3	one small crack no cracks two small cracks

TABLE 4-2

DAMAGE TO SOLAR CELL COVER GLASSES

Cracks

SAPPHIRE

Assemblage No.	Environment	Cell No.	Damage
25	24hr/50km/ambient	1 2 3	no cracks no cracks no cracks
26	72hr/50km/ambient	1 2 3	no cracks no cracks no cracks
27	24hr/100km/ambient	1 2 3	no cracks no cracks no cracks
28	72hr/100km/ambient	1 2 3	one crack no cracks no cracks
29	24hr/50km/245°K	1 2 3	no cracks no cracks two minor cracks
30	72hr/50km/diurnal	1 2 3	no cracks no cracks no cracks

TABLE 4-2

DAMAGE TO SOLAR CELL COVER GLASSES

Cracks

SAPPHIRE

Assemblage No.	Environment	Cell No.	Damage
31	72hr/100km/245°K	1 2 3	no cracks no cracks no cracks
32	72hr/50km/245°K	1 2 3	no cracks one marginal & several interior crack no cracks
33	24hr/50km/diurnal	1 2 3	no cracks no cracks no cracks
34	24hr/50km/245°K	1 2 3	no cracks no cracks no cracks
35	72hr/100km/diurnal	1 2 3	no cracks no cracks no cracks
36	24hr/100km/diurnal	1 2 3	five cracks no cracks interior cracks

TABLE 4-2

DAMAGE TO SOLAR CELL COVER GLASSES

Cracks

SAPPHIRE

Assemblage No.	Environment	Cell No.	Damage
73	not used		
74	24hr/50km/ambient	1 2 3	one crack two cracks no cracks
75	72hr/100km/ambient	1 2 3	no cracks no cracks no cracks
76	72hr/50km/ambient	1 2 3	small crack no cracks no cracks
77	72hr/100km/diurnal	1 2 3	no cracks no cracks no cracks
78	not used		

TABLE 4-2

DAMAGE TO SOLAR CELL COVER GLASSES

Cracks

SAPPHIRE

Assemblage No.	Environment	Cell No.	Damage
79	72hr/50km/245°K	1 2 3	two interior cracks no cracks no cracks
80	24hr/50km/diurnal	1 2 3	one short crack no cracks no cracks
81	72hr/50km/diurnal	1 2 3	few cracks few cracks few cracks
82	24hr/100km/245°K	1 2 3	no cracks one crack no cracks
83	24hr/100km/diurnal	1 2 3	no cracks one crack no cracks
84	72hr/100km/245°K	1 2 3	no cracks no cracks minor cracks

TABLE 4-3

DAMAGE TO SOLAR CELL ASSEMBLAGES

UNBONDING OF COVER GLASSES

CORNING No. 0211 Microsheet

Assemblage No.	Environment	Cell No.	Damage
1	24hr/100km/diurnal	3	East edge
8	72hr/100km/245°K	3	East edge and SE corner
9	72hr/50km/245°K	3	East edge, S portion
12	72hr/100km/diurnal	3	two small, circular interior areas
50	24hr/50km/ambient	1 2	east edge, S part east edge, 15%

TABLE 4-3

DAMAGE TO SOLAR CELL ASSEMBLAGES

UNBONDING OF COVER GLASSES

CORNING No. 0211 Microsheet

Assemblage No.	Environment	Cell No.	Damage
53	72hr/100km/diurnal	1	SE corner
55	72hr/50km/245°K	1 2 3	East edge, 10% SW corner 100% unbonded
56	24hr/50km/diurnal	1	West edge, 70%
59	24hr/100km/diurnal	1	East edge, 40%

TABLE 4-4

DAMAGE TO SOLAR CELL ASSEMBLAGES

UNBONDING OF COVER GLASSES

SAPPHIRE

Assemblage No.	Environment	Cell No.	Damage
25	24hr/50km/ambient	2	East edge, 60%
26	72hr/50km/ambient	2	East edge, N portion, 30%
27	24hr/100km/ambient	3	East edge
28	72hr/100km/ambient	1	East edge, 10%
29	24hr/50km/245°K	1	East edge, 10%
		3	East edge, 40%
30	72hr/50km/diurnal	1	East edge, 75%
		3	East edge, 85%

TABLE 4-4

DAMAGE TO SOLAR CELL ASSEMBLAGES

UNBONDING OF COVER GLASSES

SAPPHIRE

Assemblage No.	Environment	Cell No.	Damage
31	72hr/100km/245°K	1 2 3	100% unbonded East edge and NW corner East edge
32	72hr/50km/245°K	1 2 3	East edge East edge, 60% East edge
33	24hr/50km/diurnal	1 2 3	East edge 100% unbonded 100% unbonded
34	24hr/100km/245°K	3	East edge
35	72hr/100km/diurnal	1 2 3	65% East edge East edge, 50%
36	24hr/100km/diurnal	1 2 3	East edge, N portion, 35% 80% East edge, N portion, 50%

TABLE 4-4

DAMAGE TO SOLAR CELL ASSEMBLAGES

UNBONDING OF COVER GLASSES

SAPPHIRE

Assemblage No.	Environment	Cell No.	Damage
73	Not used		
74	24hr/50km/ambient	1 2	East edge, S portion, 40% West edge, S portion, 55%
75	72hr/100km/ambient		No unbonding
76	72hr/50km/ambient		No unbonding
77	72hr/100km/diurnal	1 2	West edge, S portion, 65% 100% unbonded
78	Not used		

TABLE 4-4

DAMAGE TO SOLAR CELL ASSEMBLAGES

UNBONDING OF COVER GLASSES

SAPPHIRE

Assemblage No.	Environment	Cell No.	Damage
79	72hr/50km/245°K	1 2	East edge, S portion, 50% East edge
80	24hr/50km/diurnal	1 2 3	East half, 35% East edge, 75% West edge, 60%
81	72hr/50km/diurnal	1 2 3	East edge East half, 25% East edge, 75%
82	24hr/100km/245°C	1	East edge, 75%
83	24hr/100km/diurnal	1 2	East half, 45% East edge, 75%
84	72hr/100km/245°K	1 2 3	100% unbonded 100% unbonded East edge, N portion, 35%

TABLE 4-5

MICROSHEET COVER GLASS CRACKING VS. ENVIRONMENT

Total microsheet cover glasses tested: 66

Total microsheet cover glasses cracked: 37 or 56.1%

Environment	Nr. tested	Nr. cracked	% failure
Ambient T.	21	8	38.1
245°K.	21	15	71.4
Diurnal range, T.	24	14	58.3
Amb., 24 hrs.	9	2	22.2
Amb., 72 hrs.	12	6	50.0
245°K., 24 hrs.	9	5	55.5
245°K., 72 hrs.	12	10	83.3
Diur., 24 hrs.	12	8	66.7
Diur., 72 hrs.	12	6	50.0
Amb., 50 km/hr.	12	5	41.6
Amb., 100 km/hr.	9	3	33.3
245°K., 50 km/hr.	9	8	88.8
245°K., 100 km/hr.	12	7	58.3
Diur., 50 km/hr.	12	6	50.0
Diur., 100 km/hr.	12	8	66.7
Amb., 24 hrs., 50 km/hr.	6	2	33.3
Amb., 24 hrs., 100 km/hr.	3	0	0.0
Amb., 72 hrs., 50 km/hr.	6	3	50.0
Amb., 72 hrs., 100 km/hr.	6	3	50.0
245°K., 24 hrs., 50 km/hr.	3	3	100.0
245°K., 24 hrs., 100 km/hr.	6	2	33.3
245°K., 72 hrs., 50 km/hr.	6	5	83.3
245°K., 72 hrs., 100 km/hr.	6	5	83.3
Diur., 24 hrs., 50 km/hr.	6	4	66.7
Diur., 24 hrs., 100 km/hr.	6	4	66.7
Diur., 72 hrs., 50 km/hr.	6	2	33.3
Diur., 72 hrs., 100 km/hr.	6	4	66.7

TABLE 4-6

SAPPHIRE COVER GLASS CRACKING VS. ENVIRONMENT

Total sapphire cover glasses tested: 66

Total sapphire cover glasses cracked: 16 or 24.2%

Environment	Nr. tested	Nr. cracked	% failure
Ambient T	21	4	19.0
245°K	21	5	23.8
Diurnal range, T.	24	7	29.2
Amb., 24 hrs.	9	2	22.2
Amb., 72 hrs.	12	2	16.7
245°K., 24 hrs.	9	2	22.2
245°K., 72 hrs.	12	3	25.0
Diur., 24 hrs.	12	4	33.3
Diur., 72 hrs.	12	3	25.0
Amb., 50 km/hr.	12	3	25.0
Amb., 100 km/hr.	9	1	11.1
245°K., 50 km/hr.	12	3	25.0
245°K., 100 km/hr.	9	2	22.2
Diur., 50 km/hr.	12	4	33.3
Diur., 100 km/hr.	12	3	25.0
Amb., 24 hrs., 50 km/hr.	6	2	33.3
Amb., 24 hrs., 100 km/hr.	3	0	0.0
Amb., 72 hrs., 50 km/hr.	6	1	16.7
Amb., 72 hrs., 100 km/hr.	6	1	16.7
245°K., 24 hrs., 50 km/hr.	6	1	16.7
245°K., 24 hrs., 100 km/hr.	3	1	33.3
245°K., 72 hrs., 50 km/hr.	6	2	33.3
245°K., 72 hrs., 100 km/hr.	6	1	16.7
Diur., 24 hrs., 50 km/hr.	6	1	16.7
Diur., 24 hrs., 100 km/hr.	6	3	50.0
Diur., 72 hrs., 50 km/hr.	6	3	50.0
Diur., 72 hrs., 100 km/hr.	6	0	0.0

TABLE 4-7

MICROSHEET COVER GLASS UNBONDING VS. ENVIRONMENT

Total microsheet cover glasses tested: 66

Total microsheet cover glasses unbonded: 12 or 18.2%

Environment	Nr. tested	Nr. unbonded	% failure
Ambient T.	21	2	9.5
245°K.	21	5	23.8
Diurnal range, T.	24	5	20.8
Amb., 24 hrs.	9	2	22.2
Amb., 72 hrs.	12	0	0.0
245°K., 24 hrs.	9	0	0.0
245°K., 72 hrs.	12	5	41.7
Diur., 24 hrs.	12	3	25.0
Diur., 72 hrs.	12	2	16.7
Amb., 50 km/hr.	9	2	22.2
Amb., 100 km/hr.	12	0	0.0
245°K., 50 km/hr.	9	4	44.4
245°K., 100 km/hr.	12	1	8.3
Diur., 50 km/hr.	12	1	8.3
Diur., 100 km/hr.	12	4	33.3
Amb., 24 hrs., 50 km/hr.	6	2	33.3
Amb., 24 hrs., 100 km/hr.	3	0	0.0
Amb., 72 hrs., 50 km/hr.	6	0	0.0
Amb., 72 hrs., 100 km/hr.	6	0	0.0
245°K., 24 hrs., 50 km/hr.	6	0	0.0
245°K., 24 hrs., 100 km/hr.	3	0	0.0
245°K., 72 hrs., 50 km/hr.	6	4	66.7
245°K., 72 hrs., 100 km/hr.	6	1	16.7
Diur., 24 hrs., 50 km/hr.	6	1	16.7
Diur., 24 hrs., 100 km/hr.	6	2	33.3
Diur., 72 hrs., 50 km/hr.	6	0	0.0
Diur., 72 hrs., 100 km/hr.	6	2	33.3

TABLE 4-8

SAPPHIRE COVER GLASS UNBONDING VS. ENVIRONMENT

Total sapphire cover glasses tested: 66

Total sapphire cover glasses unbonded: 42 or 63.5%

Environment	Nr. tested	Nr. unbonded	% failure
Ambient T.	21	6	45.7
245°K.	21	15	71.4
Diurnal range, T.	24	21	87.5
Amb., 24 hrs.	9	4	44.4
Amb., 72 hrs.	12	2	16.7
245°K., 24 hrs.	9	4	44.4
245°K., 72 hrs.	12	11	91.6
Diur., 24 hrs.	12	11	91.6
Diur., 72 hrs.	12	10	83.3
Amb., 50 km/hr.	9	4	44.4
Amb., 100 km/hr.	12	2	16.7
245°K., 50 km/hr.	9	7	77.7
245°K., 100 km/hr.	12	8	66.7
Diur., 50 km/hr.	12	11	91.6
Diur., 100 km/hr.	12	10	83.3
Amb., 24 hrs., 50 km/hr.	6	3	50.0
Amb., 24 hrs. 100 km/hr.	3	1	33.3
Amb., 72 hrs., 50 km/hr.	6	1	16.7
Amb., 72 hrs., 100 km/hr.	6	1	16.7
245°K., 24 hrs., 50 km/hr.	3	2	66.7
245°K., 24 hrs., 100 km/hr.	6	2	33.3
245°K., 72 hrs., 50 km/hr.	6	5	83.3
245°K., 72 hrs., 100 km/hr.	6	6	100.0
Diur., 24 hrs., 50 km/hr.	6	6	100.0
Diur., 24 hrs., 100 km/hr.	6	5	83.3
Diur., 72 hrs., 50 km/hr.	6	5	83.3
Diur., 72 hrs., 100 km/hr.	6	5	83.3

SECTION 5

SOLAR CELL OUTPUTS

5.1 INTRODUCTION

A procedure for the determination of reduction in electrical power output of solar cell assemblages following subjection to dust storms was developed. A standardized tungsten lamp was used as a source of illumination. By using a number of different load resistors a wide range of current-voltage pairs was produced. From the current-voltage data obtained, curves representative of power output characteristics of the solar cells were plotted. The data were analyzed and represented by I-V curves. Three sets of curves were produced for each solar cell assemblage: (1) in its original condition as received from JPL, (2) after subjecting to "dust storm" in specified environment, and (3) after removing dust and cleaning surfaces of protective covers. The three sets of measurements were made under similar conditions.

5.2 SOURCE OF ILLUMINATION

A tungsten-iodine lamp was used as a source of illumination for the solar cell measurements because of its high color temperature, high intensity, stability and availability in calibrated form. The lamp procured for this purpose is

the type used by the National Bureau of Standards as the "Standard of Spectral Irradiance". It is a 1000W lamp that consists of a coiled tungsten filament (3000K) contained in a 1 x 7 cm quartz envelope (Stair and others, 1963). The lamp and its certificate of calibration were obtained from Eppley Laboratory, Newport, Rhode Island. It was calibrated over the wavelength interval 250nm to 2500nm, based on the radiance of a Planckian radiator.

The lamp was operated from a Sorensen A.C. Voltage Regulator during all measurements, and a Variac autotransformer was used to adjust the operating current to its rated value of 8.3 amperes. Under these conditions the output of the standard will change less than 1% per hundred hours of operation.

5.3 ADJUSTMENT OF THE ILLUMINATION SOURCE TO SIMULATE THE SOLAR ENVIRONMENT AT MARS

The electrical output characteristics of solar cells to illumination in the testing environment should approximate those that would be produced on the surface of Mars. Because natural sunlight and tungsten light have different spectral energy distributions, the response of a cell will differ under the two sources. Because calculation of the electrical output of a cell to the two types of illumination

would necessitate a point-by-point match of the cell's spectral response and the spectral emission of the source, an alternate method was used in which the absolute measurement of the electrical output of the cells is not required.

A silicon solar cell similar to the type supplied by JPL for the experiments was illuminated by natural sunlight on a clear day at ground elevation at Lubbock, Texas. The short-circuit current of the cell was measured and recorded. This cell was then placed on the test bench and the cell to lamp distance adjusted to provide the identical short-circuit current. The cell to lamp distance was then increased by the ratio of the mean radius of the orbit of Mars to the mean radius of the orbit of the Earth, 228×10^6 km to 149×10^6 km, respectively. This reduced level of illumination should produce a very approximately similar cell response as the illumination on the surface of Mars, not taking into account the significant difference in relative photon scattering by Martian atmospheric conditions. Absolute light intensity was not measured.

5.4 MEASUREMENT OF SOLAR CELL AMPERE-VOLT CHARACTERISTICS

A silicon solar cell generally exhibits a nonlinear volt-ampere characteristic which is an apparent function of both the physical construction of the cell and the specific

condition on input radiation. In order to obtain an I-V curve the resistance across the solar cell assemblage was varied and the resultant voltages recorded. Twenty Dale type RS-5 precision power resistors were sequentially switched across each cell by an automatically operated a Clare stepping switch which was immersed in a bath of Humble "Bayol D" potentiometer oil. The resistances were measured to an accuracy of 1% with a Hewlett-Packard 3440 A Digital Voltmeter and type 3444 A plug in. The voltages developed across the total system were recorded by a Honeywell Brown Potentiometric Recorder, and subsequently transferred to punched cards for computer analysis. The Brown recorder was calibrated using a zinc-carbon cell measured to 1/10% with a Hewlett-Packard type 3420 A Voltmeter-Ratiometer. Measurements made on individual solar cell assemblages in this manner were found to be repeatable to within an accuracy of 2%. The time interval of the switching sequence was held to under 30 seconds in order to avoid excessive heating of the cells by the tungsten lamp. Actual temperatures should have been but were not measured.

5.5 POWER OUTPUT DATA

The I-V curves for the various solar cell assemblages

(see identification in Table 5-3) are indicated on Figures 5-1 through 5-8. The statistically refined maximum power data populations are given in Tables 5-1 and 5-2.

Statistically refined refers to a process of population refinement of data. It is a technique of rejecting data which clearly do not belong to a normal data population. It is a standard procedure to refine experimental data in order to locate the main population by rejecting outlier data. The confidence limits at a 0.05 probability are presented as an estimate of the significance of the difference between means,, $\Delta\bar{x}$, between maximum power average values. It is assumed that if the confidence limit ranges do not overlap a high likelyhood of significance of $\Delta\bar{x}$ exists. The maximum powers were averaged as a part of the statistical analysis which includes the population refinement technique. The question of environmental effects was considered but statistically no effect in terms of maximum power could be discerned. In other words no separate populations with regards to various environments were discovered. On this basis we were limited to a refinement of the data on the basis of variation between cover glasses and post-wind tunnel treatment. The results of this statistical data treatment seemed satisfactory.

As the individual maximum power values obtained do not appear to have any statistical reality in the terms of tha various environments, it is felt that to construct a matrix listing individual maximum power values would be misleading. For our data it is only the average value with the confidence limits which would serve as a guide line for possible future work.

The I-V curves of the refined populations, virgin vs. sand-blasted and cleaned, in conjunction with the confidence limit data reveal permanent damage has occurred to the solar cell modules. The decrease in average maximum power is probably related to a change in optical properties of the cover glasses. The I-V curves indicated by Figures 5-9 and 5-10 are those obtained from the JPL solar simulator on specific solar cells and cell assemblages and may be compared with those obtained from the identical solar cell assemblages by means of the Texas Tech tungsten source. You will notice that the specimens indicated on the JPL curves also have been shown on the Texas Tech curves. A comparison of the curves as revealed by the I-V data obtained from the solar simulator and the tungsten source may thus be made.

The differences between the uncleaned, sand blasted solar cells is apparently due to variation in dust adherence.

No specific pattern was obvious or to be expected because of accidental variations in dust adherence. Identification of the modules used in each test environment is given in Table 5-3.

Variations in maximum power output values for the modules with the same type of cover glasses range over wide limits. From the figures, 5-1 through 5-8, however, it is obvious that there are definite groupings of the curves obtained from the virgin modules as well as obtained from modules which had been sand blasted and cleaned. The I-V curves representing the measurements of modules with dust not removed show a wide distribution in electrical output value. For purposes of a general analysis, however, arithmetical mean values for power output in all three conditions are meaningful. Average output values in percentages are presented in Table 5-4. The arithmetic mean values for the power output of virgin cells is assumed to be 100%.

TABLE 5-4

AVERAGE MAXIMUM POWER OUTPUT IN PERCENTAGES OF THE ORIGINAL VIRGIN CELLS

Type of Cover Glass	After dust storm		After cleaning	
	Ag mesh	JPL bus bar	Ag mesh	JPL bus bar
Microsheet	23.5	25.8	63.3	65.3
Silica	32.6	30.7	67.6	64.0
Sapphire	29.1	37.3	75.1	70.1
Integral	33.7	39.2	73.4	78.4

From the values listed in Table 5-4 it is apparent that a drop in power output due to dust adherence and actual assemblage damage in the range 60% to 80% can be expected. It appears also that the amount of dust adherence and damage varies with the cover glass material, decreasing in this order: microsheet, silica, sapphire, and integral.

Decrease in power output due to permanent damage as revealed after cleaning can be expected to range between 25% and 40%. Microsheet and silica cover glasses are more vulnerable than are those of sapphire and integral.

There are no significant differences in the amounts of dust accumulating over periods of time. From direct observations it was noted that the maximum dust coatings accumulated during the first few minutes after the dust storms started.

An analysis of the effect of the environmental conditions was made (Section 4.6). The gross effects of the cover glass materials and the interconnectors overshadowed the finer environmental effect. Table 5-5 represents a listing of the various average maximum power outputs of the solar cell assemblages in relationship to types of cover glasses and electrical interconnectors.

TABLE 5-5

EFFECTS OF COVER GLASS DAMAGE AND INTERCONNECTOR TYPES ON MAXIMUM POWER WATTAGE OUTPUT

Type of cover glass	Ag mesh			JPL Bus Bar		
	virgin	after cleaning	ΔP*	virgin	after cleaning	ΔP
Microsheet	50.5	32.0	18.5	51.15	33.4	17.73
Fused SiO_2	50.3	34.0	16.3	50.1	32.3	17.8
Sapphire	50.3	37.9	12.4	51.2	35.9	15.3
Integral	47.2	34.6	12.6	45.3	35.5	9.8

*ΔP = Decrease in maximum power output

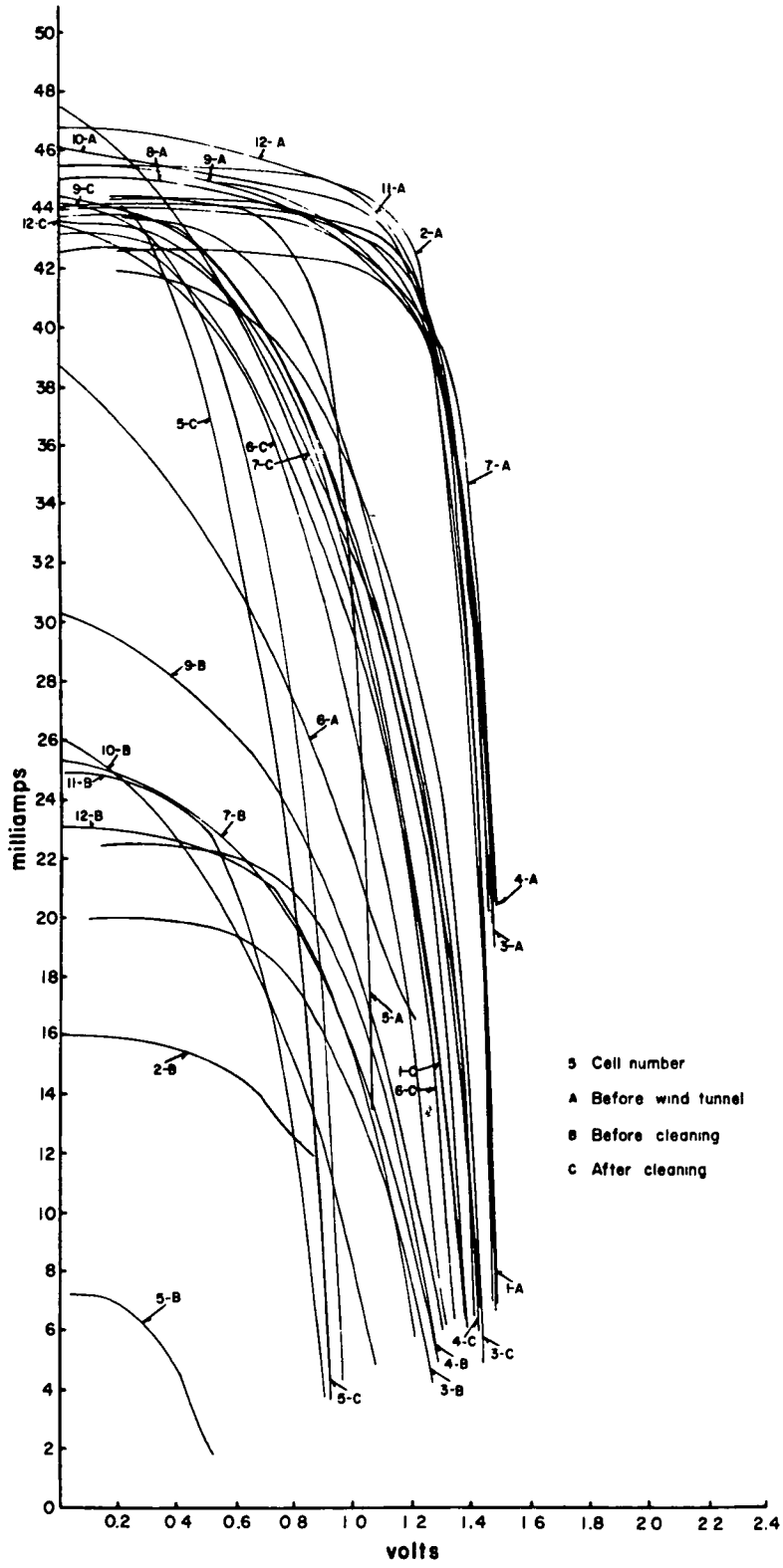

Figure 5-1. I-V Curves. Microsheet. Silver Mesh Connectors. Refer to Table 5-3 for cell number identification.

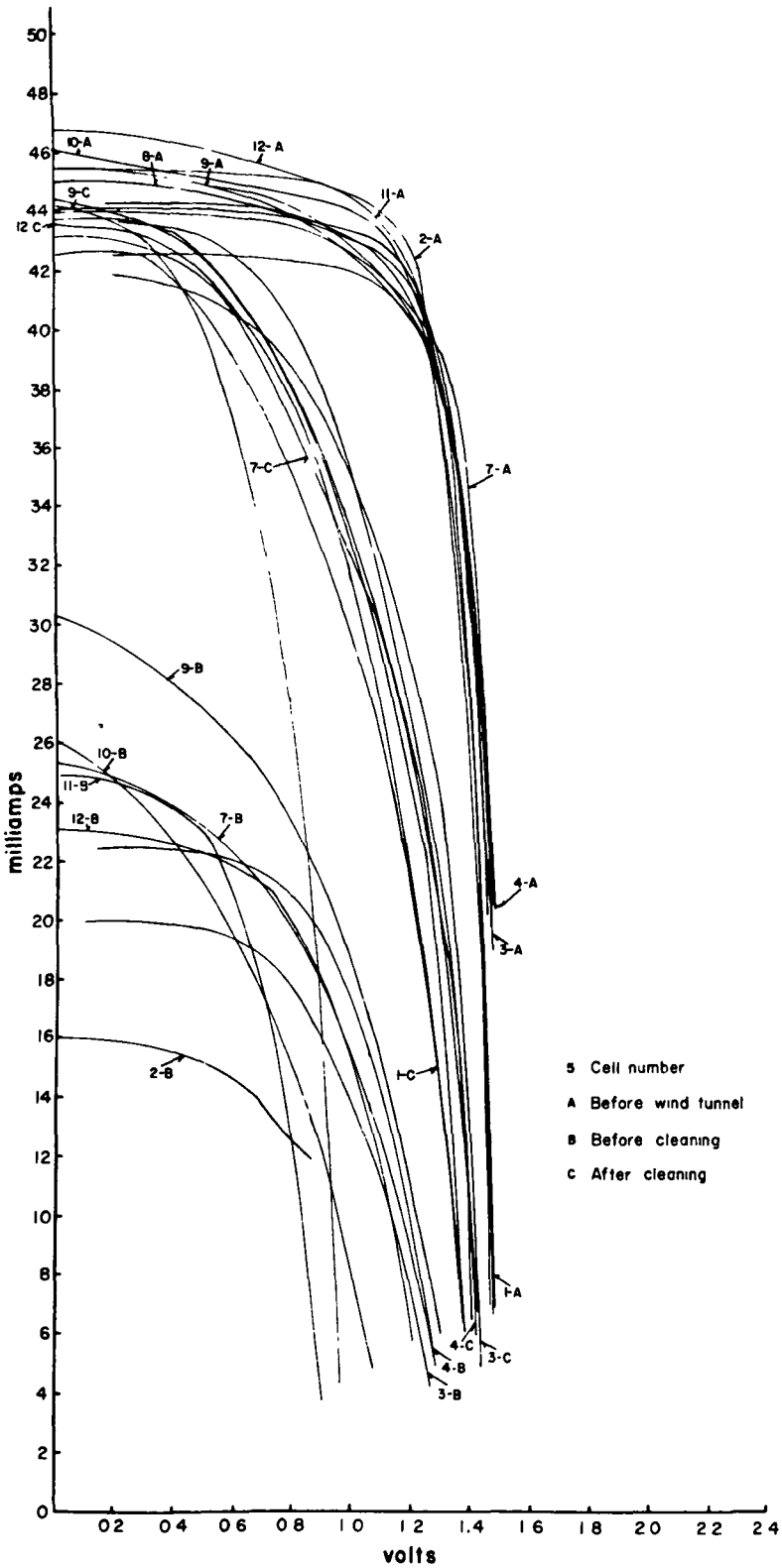

Figure 5-1 (a). Showing remaining I-V curves, after population refinement of family of curves indicated in Figure 5-1. Refer to Table 5-3 for cell number identification.

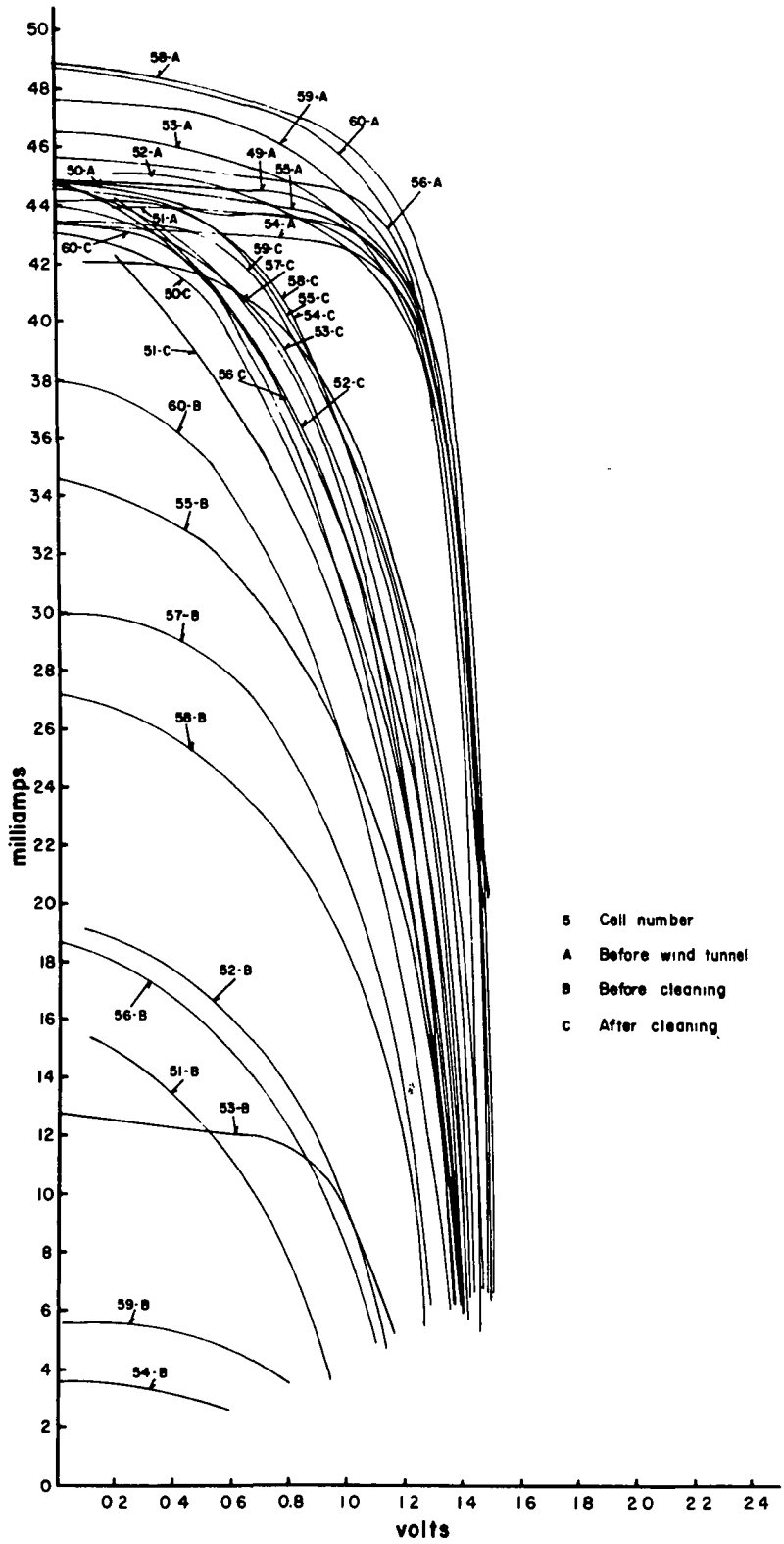

Figure 5-2. I-V Curves. Microsheet. JPL Bus Bar Connectors. Refer to Table 5-3 for cell number identification.

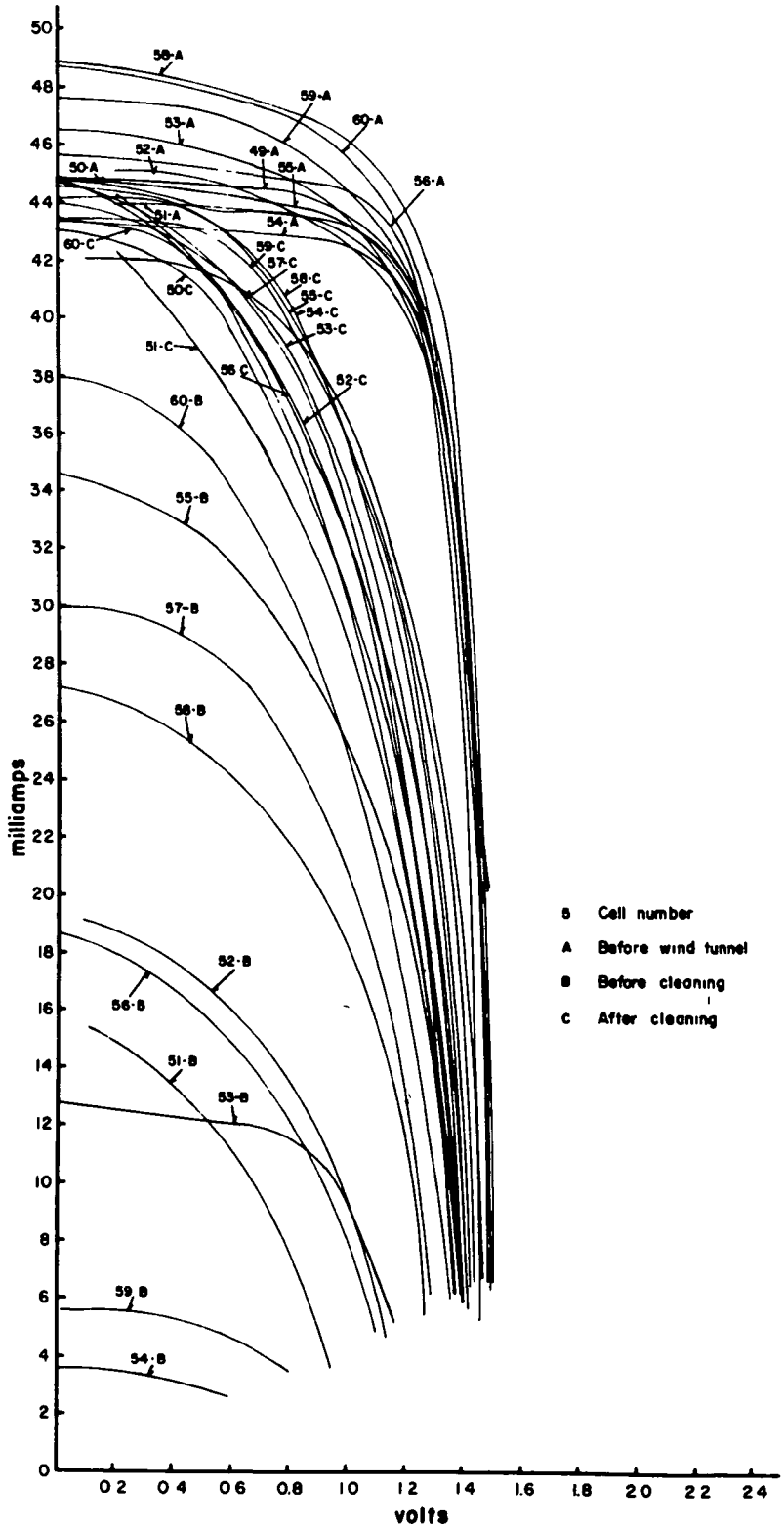

Figure 5-2 (a). Showing remaining I-V curves, after population refinement of family of curves indicated in figure 5-2. Refer to Table 5-3 for cell number identification.

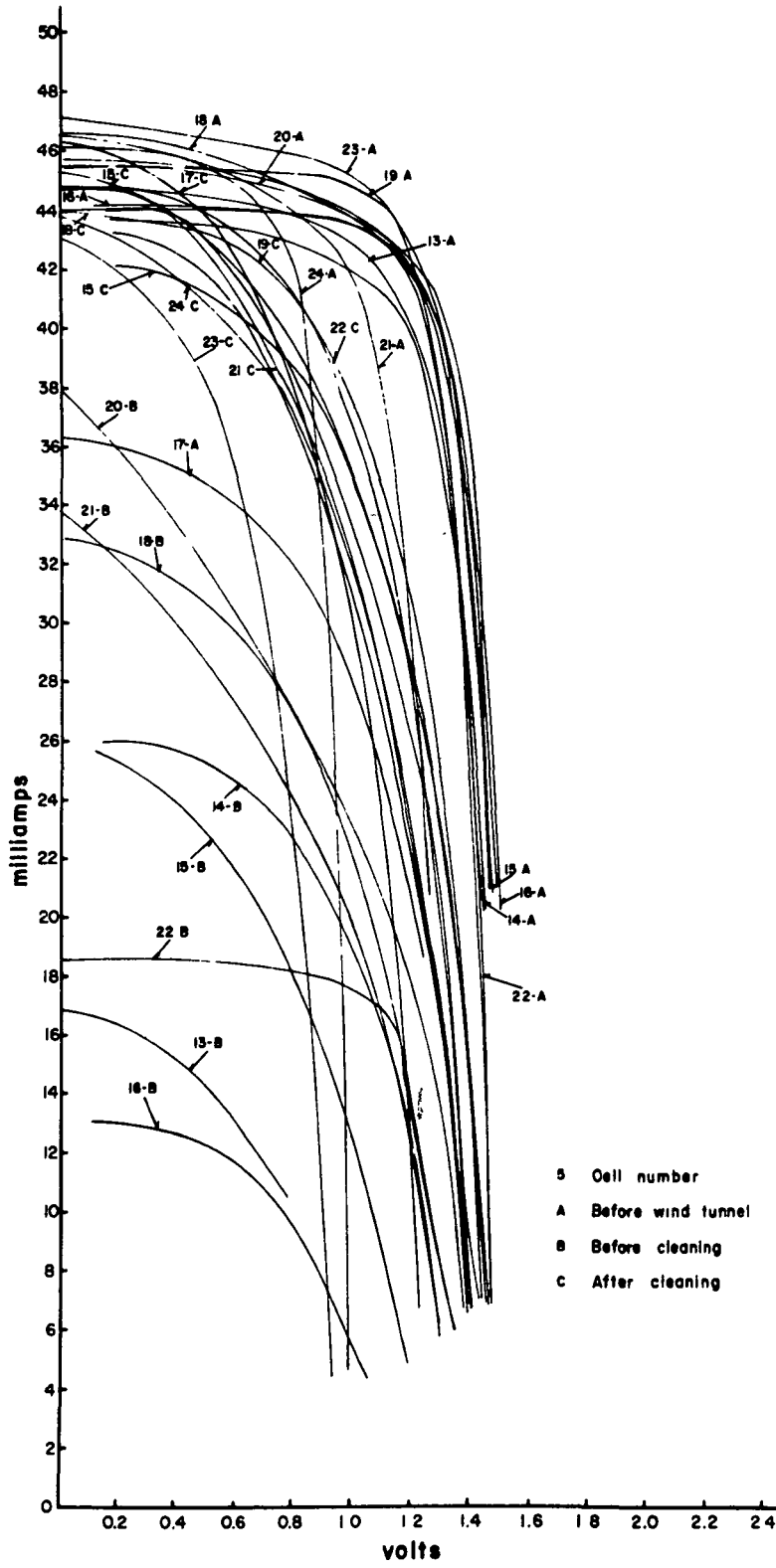

Figure 5-3. I-V Curves. Fused Silica. Silver Mesh Connectors. Refer to Table 5-3 for cell number identification.

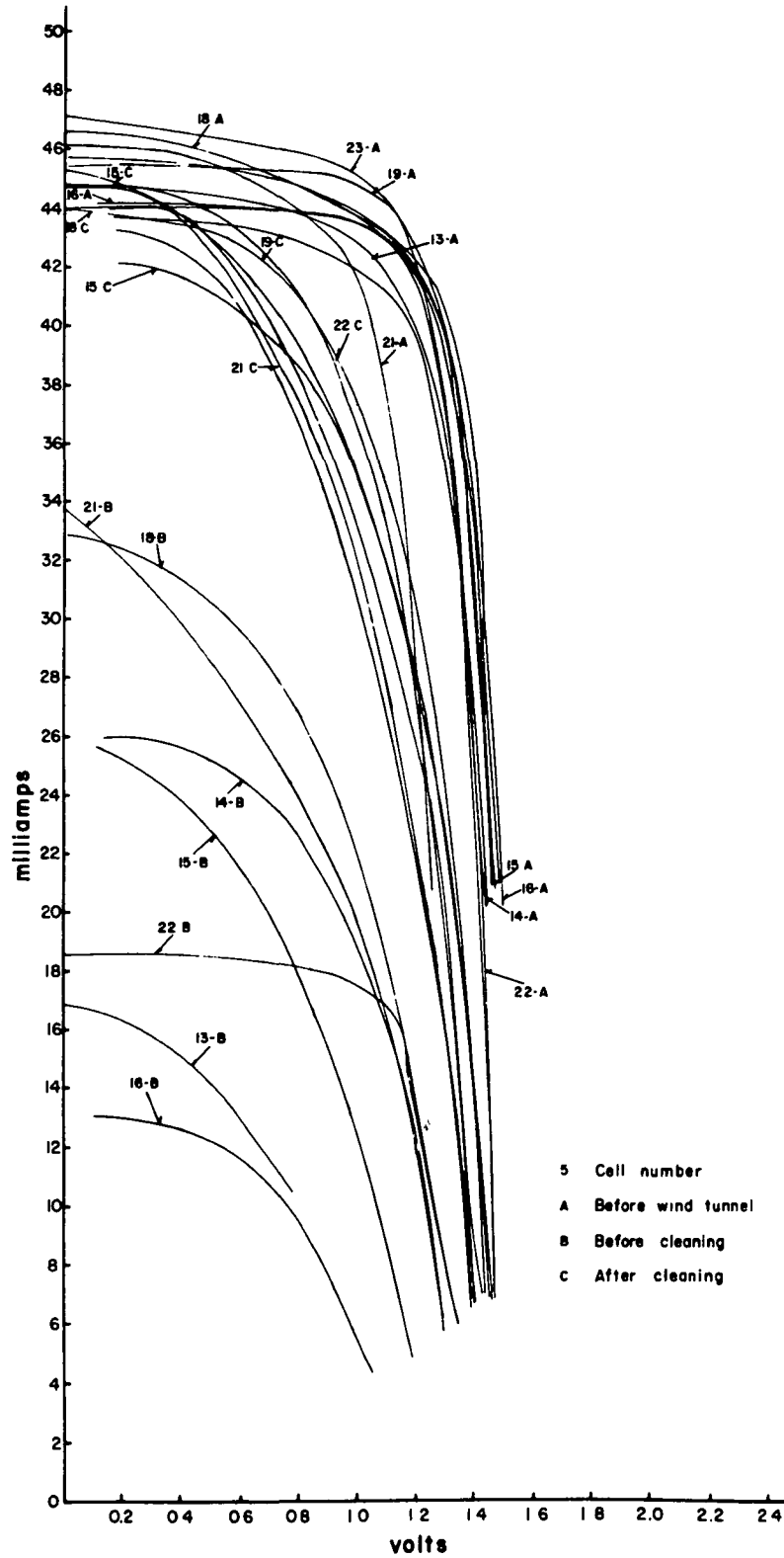

Figure 5-3 (a). Showing remaining I-V curves, after population refinement of family of curves indicated in Figure 5-3. Refer to Table 5-3 for cell number identification.

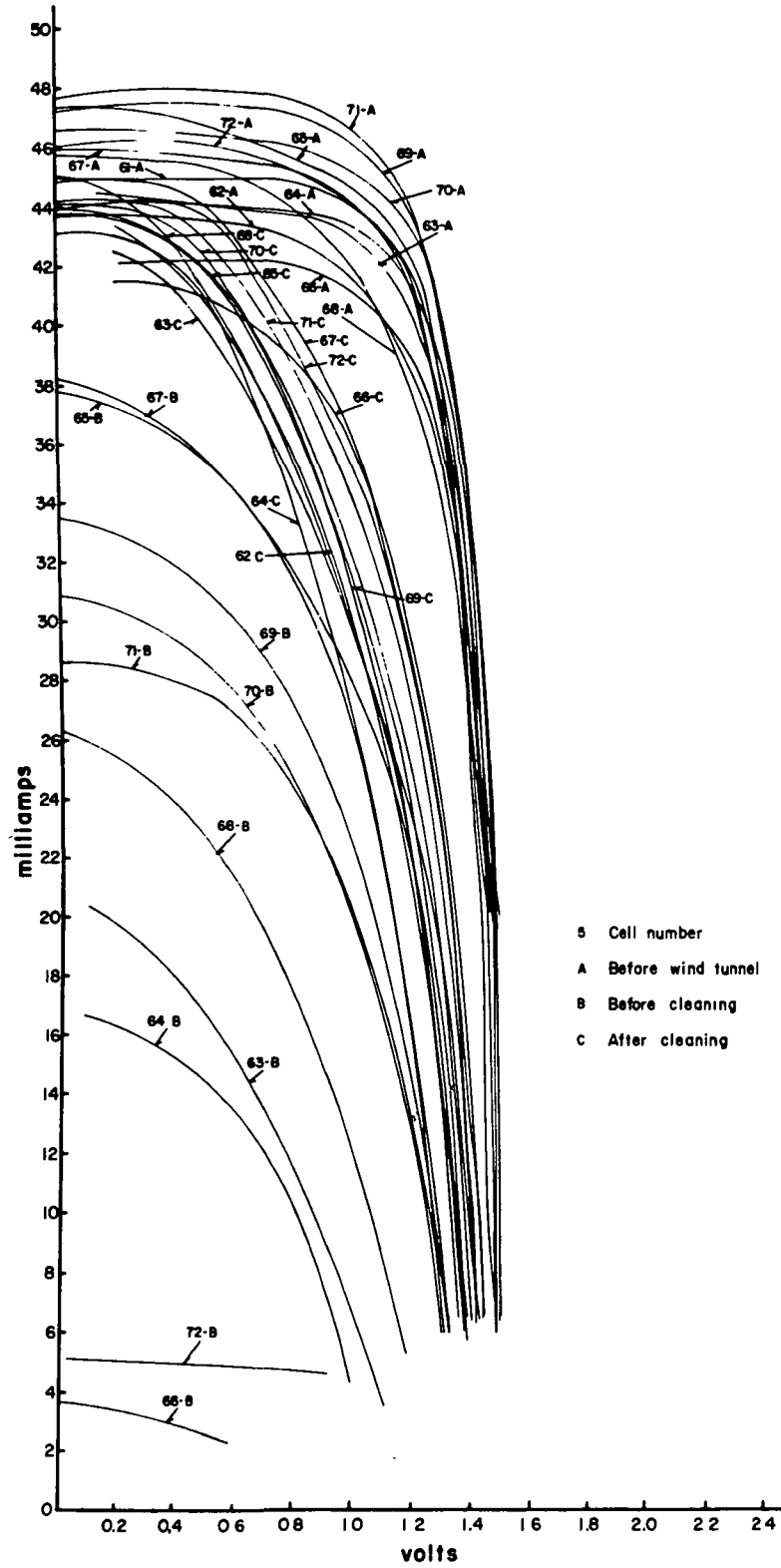

Figure 5-4. I-V Curves. Fused Silica. JPL Bus Bar Connectors. Refer to Table 5-3 for cell number identification.

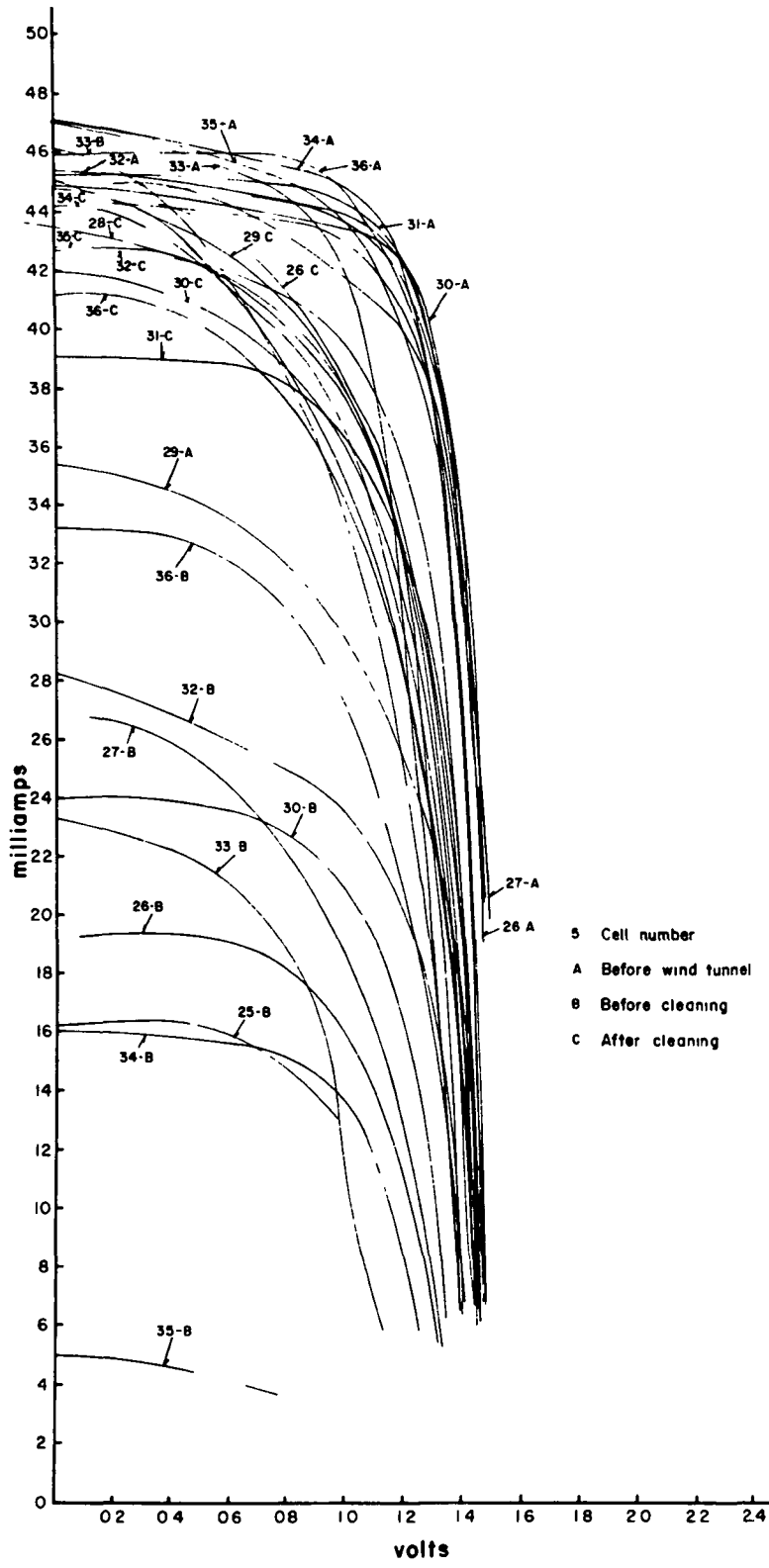

Figure 5-5. I-V Curves. Sapphire. Silver Mesh Connectors. Refer to Table 5-3 for cell number identification.

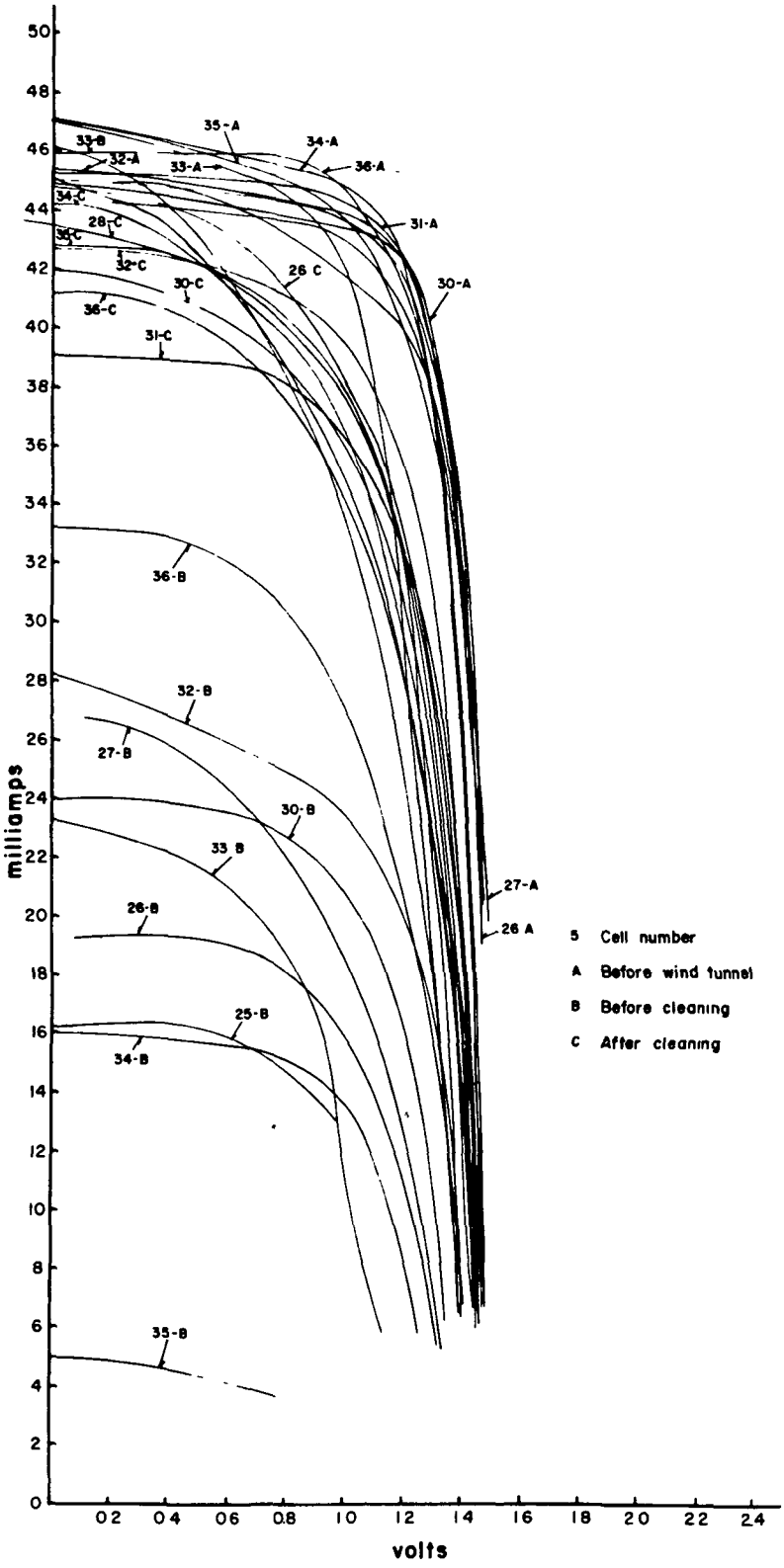

Figure 5-5 (a). Showing remaining I-V curves, after population refinement of family of curves indicated in Figure 5-5. Refer to Table 5-3 for cell number identification.

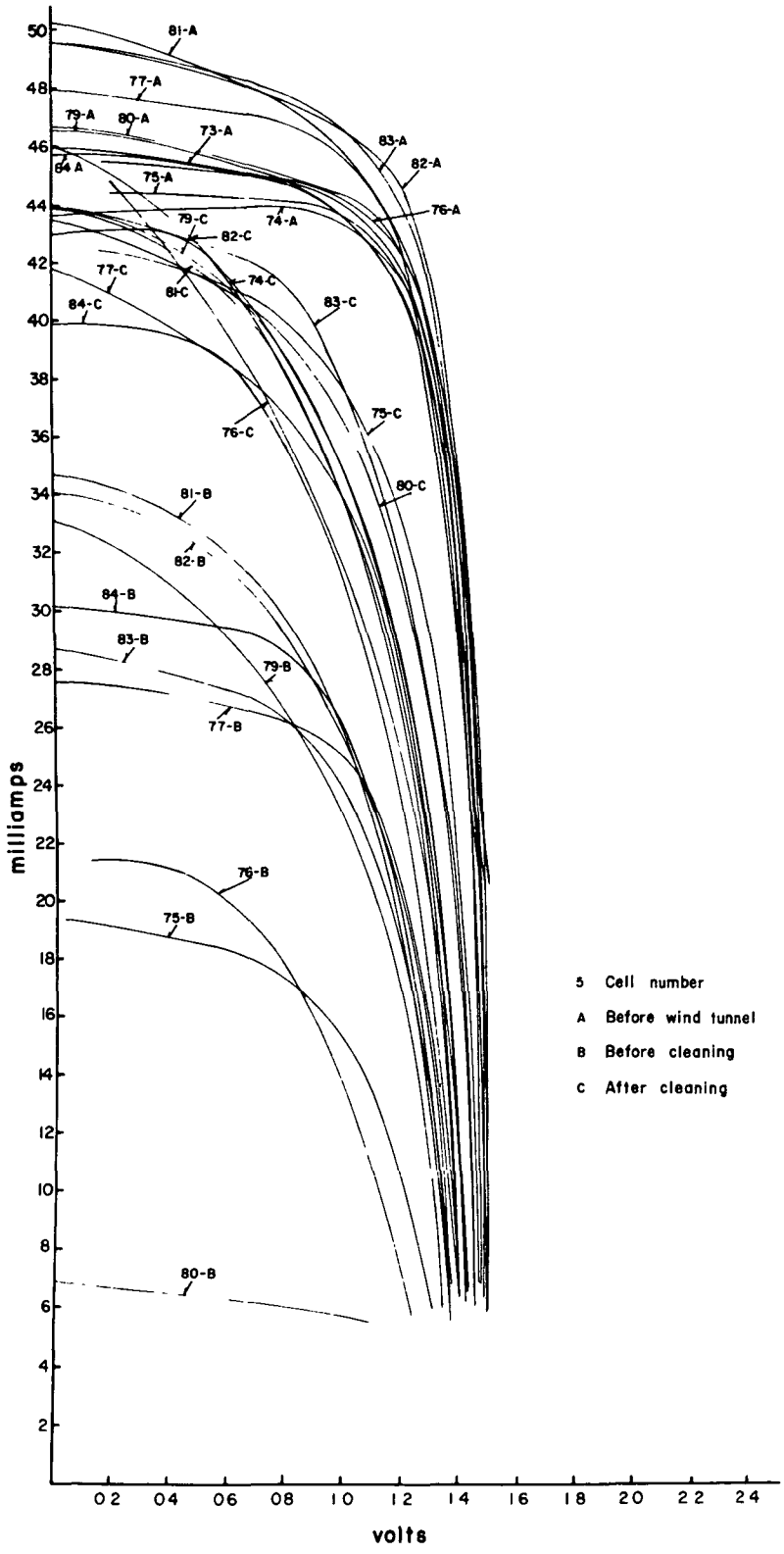

Figure 5-6. I-V Curves. Sapphire. JPL Bus Bar Connectors. Refer to Table 5-3 for cell number identification.

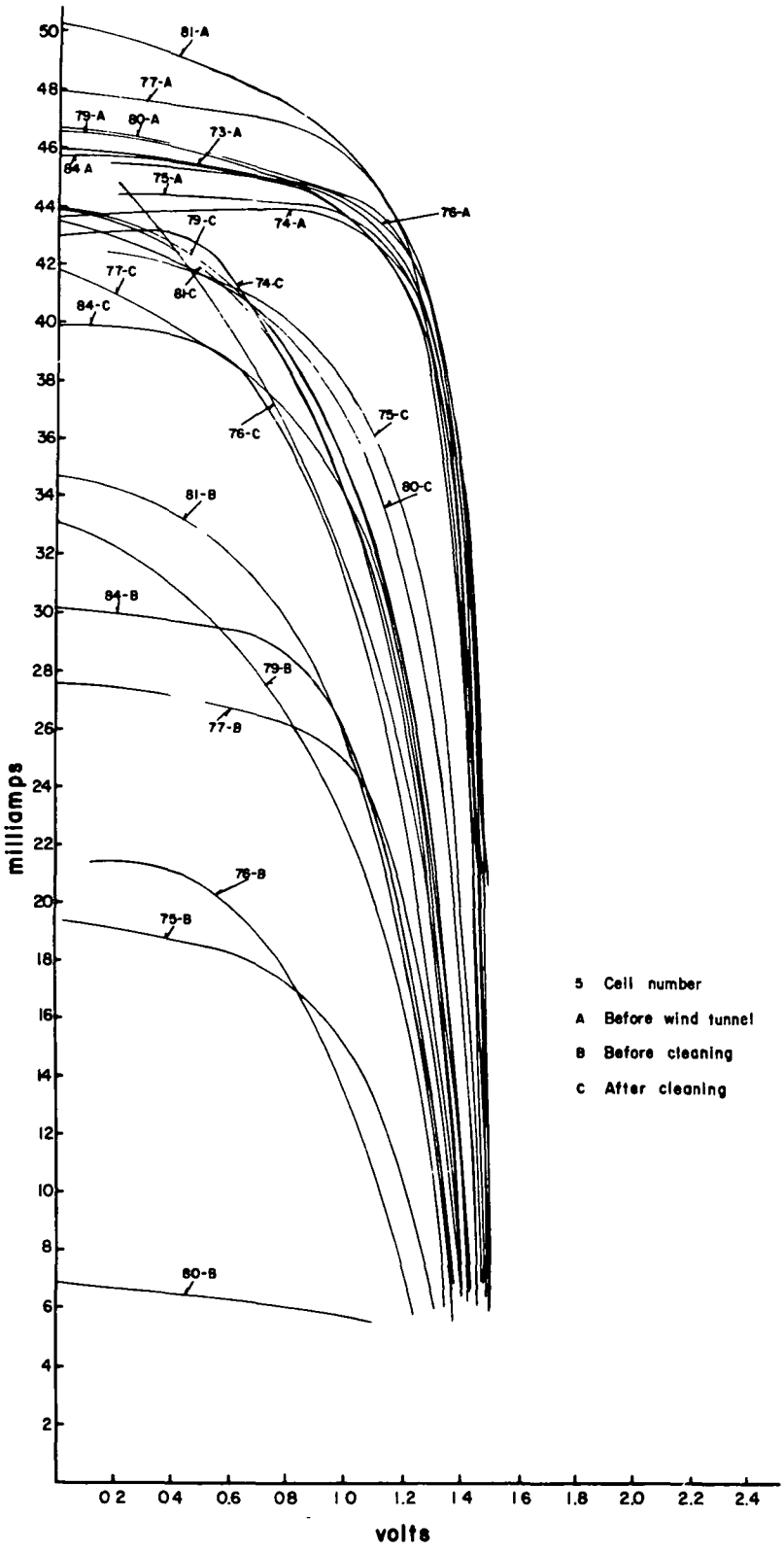

Figure 5-6 (a). Showing remaining I-V curves, after population refinement of family of curves indicated in Figure 5-6. Refer to Table 5-3 for cell number identification.

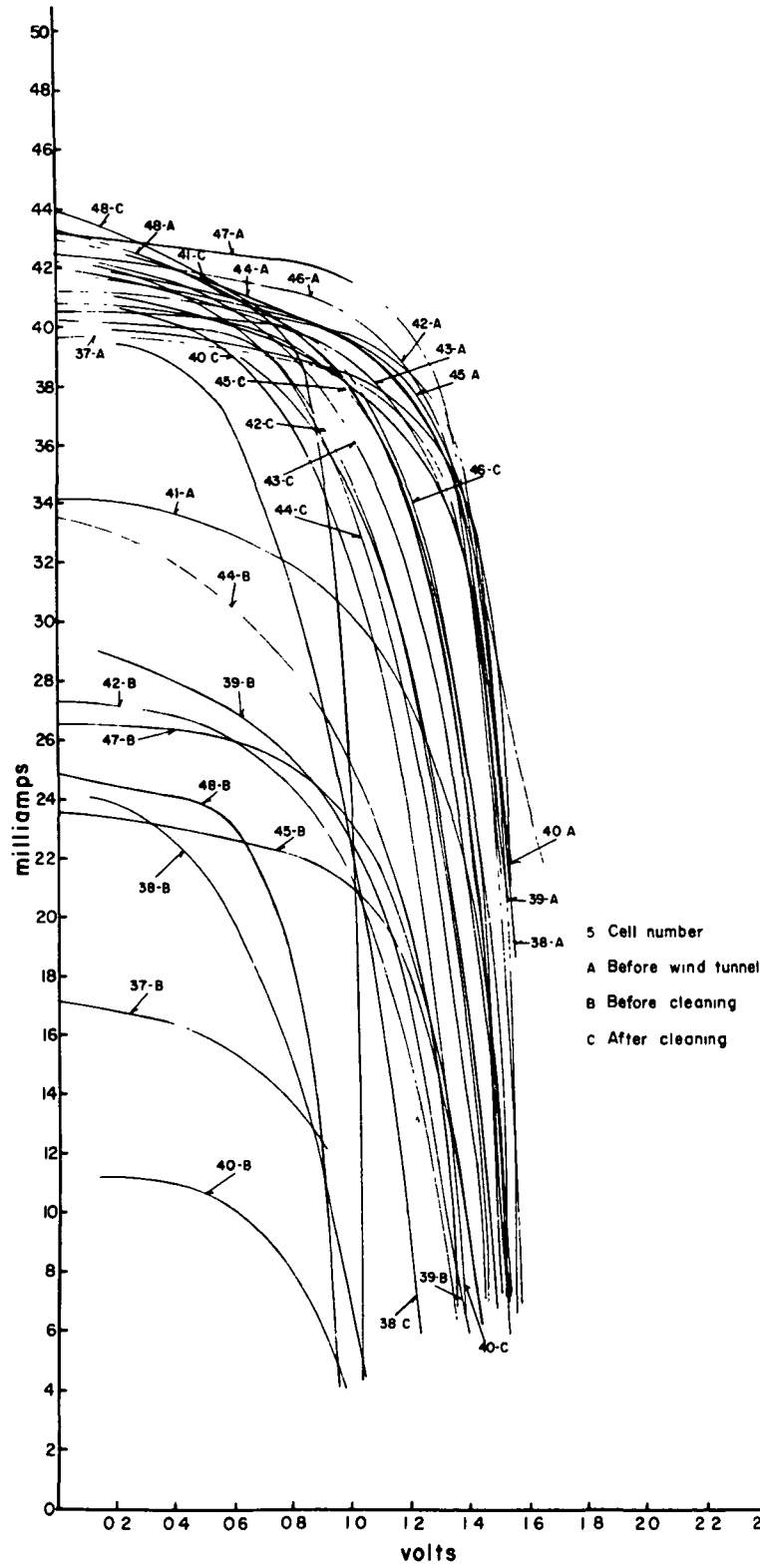

Figure 5-7. I-V Curves. Integral. Silver Mesh Connectors. Refer to Table 5-3 for cell number identification.

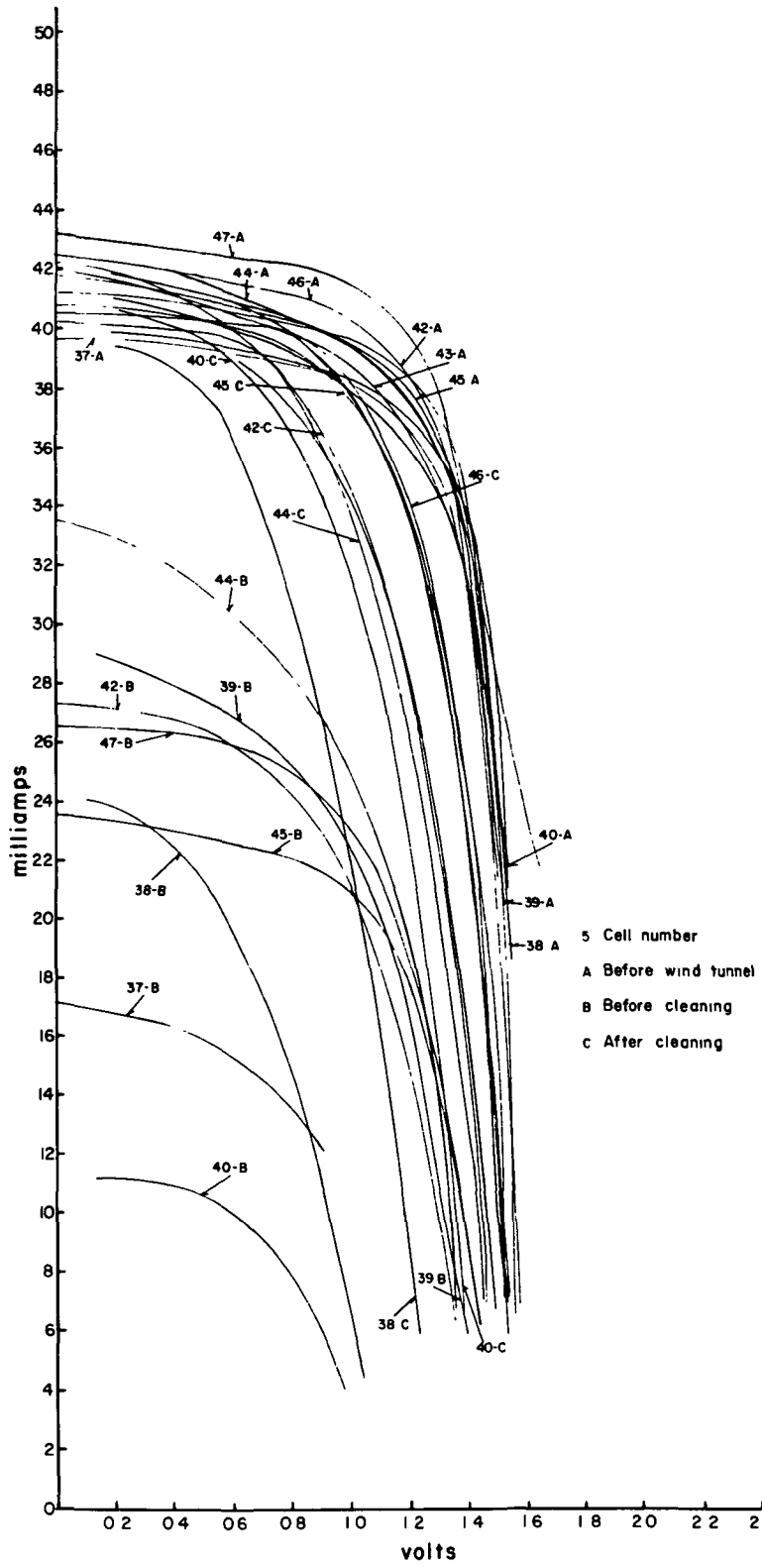

Figure 5-7 (a). Showing remaining I-V curves, after population refinement of family of curves indicated in Figure 5-7. Refer to Table 5-3 for cell number identification.

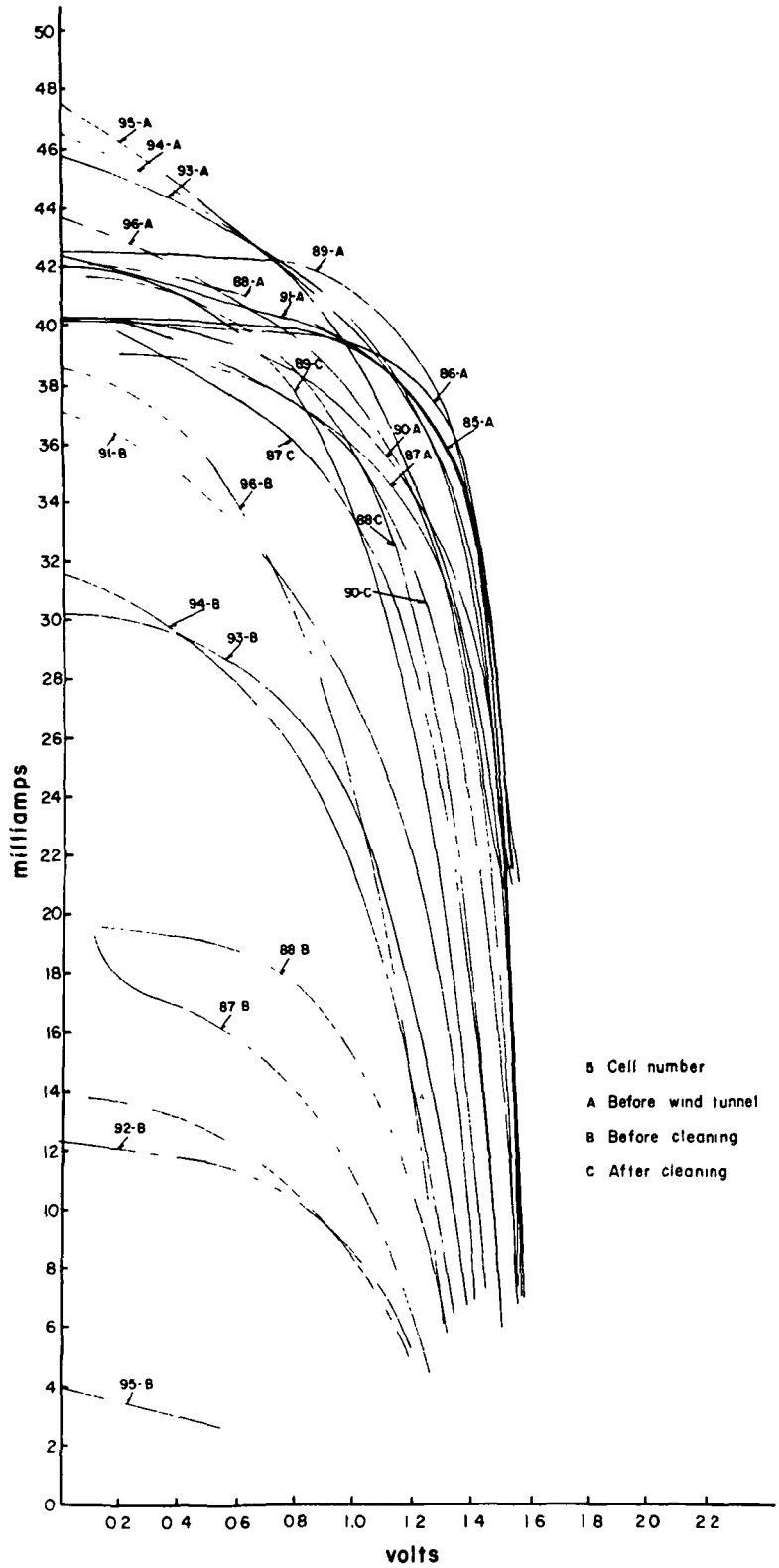

Figure 5-8. I-V Curves. Integral. JPL Bus Bar Connectors. Refer to Table 5-3 for cell number identification.

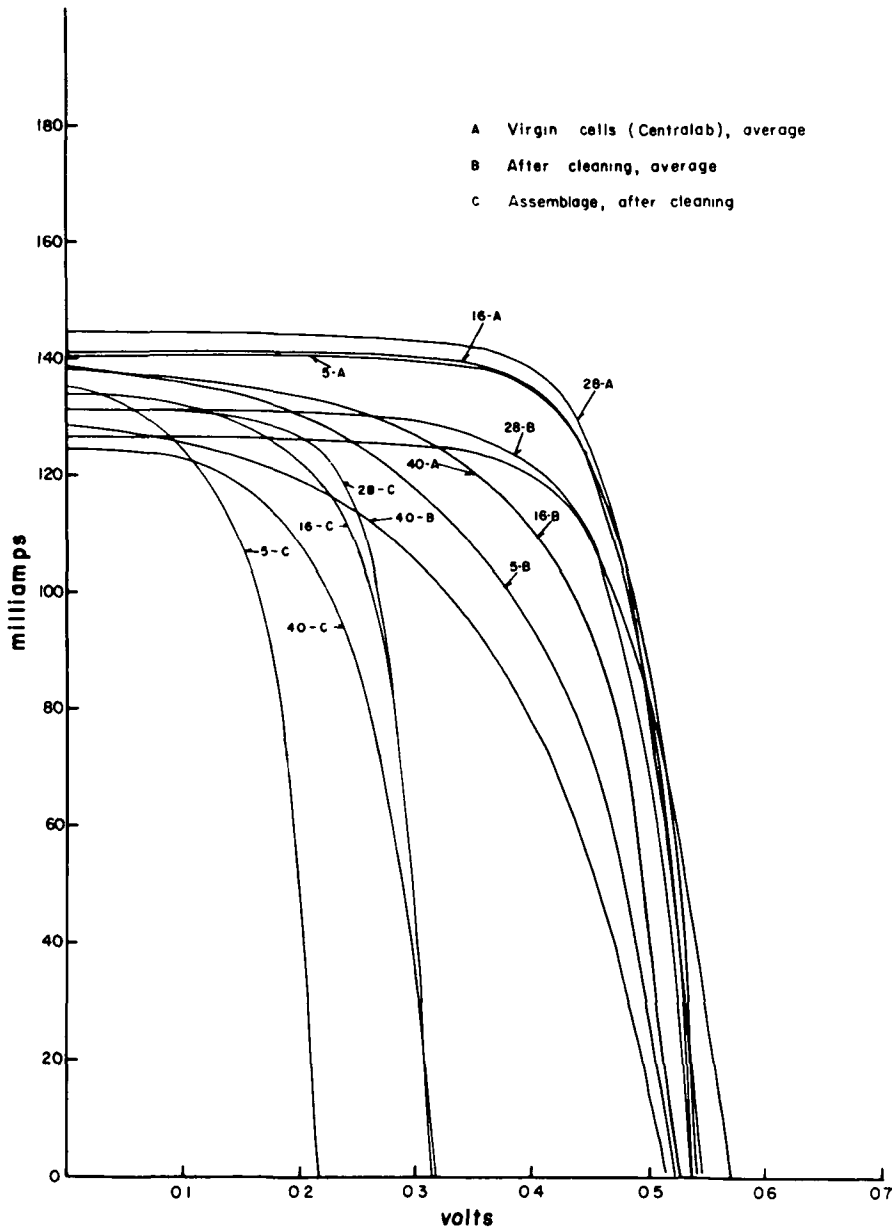

Figure 5-9. I-V curves, for solar cells with various cover glasses tested by JPL. The I-V curves indicated by the letter C represent solar cell assemblages. The voltages for these curves should be multiplied by five. Refer to Table 5-3 for cell number identification.

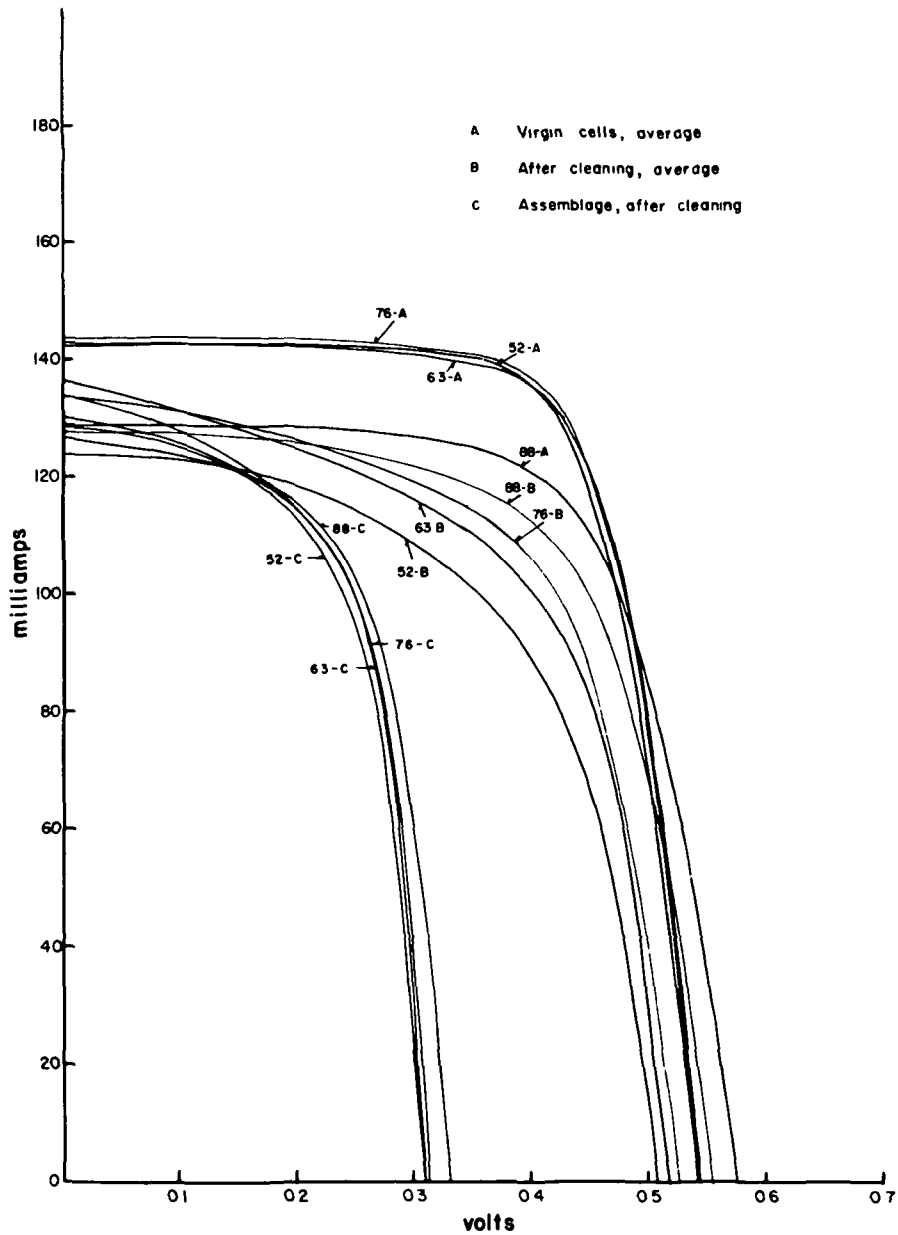

Figure 5-10. I-V curves, for solar cells with various cover glasses tested by JPL. The I-V curves indicated by the letter C represent solar cell assemblages. The voltages for these curves should be multiplied by five. Refer to Table 5-3 for cell number identification.

TABLE 5-1

MAXIMUM POWER OF SOLAR CELL MODULES

Silver Mesh Connectors

CELL TYPE: MICROSHEET BEFORE SANDBLASTING

Cell No.	Maximum Power in Milli-watts
1	50.53
2	51.24
3	49.62
4	50.31
7	51.63
8	50.08
9	50.49
10	50.59
11	50.25
12	50.62

Arithmetic Mean = 50.5359 Standard Deviation = 0.57

Variance = 0.32 Confidence Limit = 0.4285

CELL TYPE: MICROSHEET AFTER SANDBLASTING BUT BEFORE CLEANING

Cell No.	Maximum Power in Milli-watts
1	0.03
2	10.31
3	14.36
4	17.48
5	1.89
7	15.99
9	19.17
10	12.28
11	12.35
12	16.13

Arithmetic Mean = 11.9990 Standard Deviation = 6.40

Variance = 40.95 Confidence Limit = 4.8249

TABLE 5-1 Continued

CELL TYPE: MICROSHEET AFTER SANDBLASTING AND CLEANING

Cell No.	Maximum Power in Milli-watts
1	29.63
3	35.09
4	35.05
6	30.68
7	32.62
8	33.37
9	32.74
10	27.44
12	31.24

Arithmetic Mean = 31.9844 Standard Deviation = 2.51

Variance = 6.30 Confidence Limit = 2.0460

CELL TYPE: FUZED QUARTZ BEFORE SANDBLASTING

Cell No.	Maximum Power in Milli-watts
13	47.74
14	47.20
15	51.36
16	51.59
18	52.81
19	52.04
21	49.85
22	49.05
23	50.85

Arithmetic Mean = 50.2755 Standard Deviation = 1.95

Variance = 3.81 Confidence Limit = 1.5905

TABLE 5-1 Continued

CELL TYPE: FUZED QUARTZ AFTER SANDBLASTING BUT BEFORE CLEANING

Cell No.	Maximum Power in Milli-watts
13	8.24
14	19.07
15	14.34
16	7.61
18	21.78
20	23.17
21	20.12
22	17.72
23	11.74
24	20.22

Arithmetic Mean = 16.4010 Standard Deviation = 5.60

Variance = 31.32 Confidence Limit = 4.2198

CELL TYPE: FUZED QUARTZ AFTER SANDBLASTING AND CLEANING

Cell No.	Maximum Power in Milli-watts
15	30.21
16	35.18
17	36.35
18	33.08
19	36.31
21	31.73
22	37.60
24	31.87

Arithmetic Mean = 34.0412 Standard Deviation = 2.68

Variance = 7.16 Confidence Limit = 2.3912

TABLE 5-1 Continued

CELL TYPE: SAPPHIRE BEFORE SANDBLASTING

Cell No.	Maximum Power in Milli-watts
25	50.44
26	49.21
27	49.28
28	51.48
30	52.11
31	51.47
32	50.93
33	50.23
34	50.38
35	48.28
36	49.50

Arithmetic Mean = 50.3008 Standard Deviation = 1.16

Variance = 1.35 Confidence Limit = 0.8172

CELL TYPE: SAPPHIRE AFTER SANDBLASTING BUT BEFORE CLEANING

Cell No.	Maximum Power in Milli-watts
25	12.55
26	15.75
27	18.71
28	9.93
30	20.88
31	0.48
32	24.52
33	15.30
34	13.62
35	2.88
36	26.80

Arithmetic Mean = 14.6745 Standard Deviation = 8.18

Variance = 66.90 Confidence Limit = 5.7629

TABLE 5-1 Continued

CELL TYPE: SAPPHIRE AFTER SANDBLASTING AND CLEANING

Cell No.	Maximum Power in Milli-watts
26	40.24
27	35.25
28	42.17
29	39.31
30	37.28
31	38.70
32	41.93
33	33.60
34	36.38
35	38.87
36	33.42

Arithmetic Mean = 37.9227 Standard Deviation = 3.03

Variance = 9.18 Confidence Limit = 2.1348

CELL TYPE: INTEGRAL BEFORE SANDBLASTING

Cell No.	Maximum Power in Milli-watts
37	46.12
38	47.14
39	44.80
40	47.36
42	48.79
43	45.88
44	47.08
45	47.23
46	47.95
47	49.46

Arithmetic Mean = 47.1810 Standard Deviation = 1.37

Variance = 1.88 Confidence Limit = 1.0338

TABLE 5-1 Continued

CELL TYPE: INTEGRAL AFTER SANDBLASTING BUT BEFORE CLEANING

Cell No.	Maximum Power in Milli-watts
37	11.05
38	12.31
39	22.36
40	6.46
42	21.27
43	0.05
44	25.02
45	21.98
47	23.63
48	14.96

Arithmetic Mean = 15.9090 Standard Deviation = 8.35

Variance = 69.79 Confidence Limit = 6.2988

CELL TYPE: INTEGRAL AFTER SANDBLASTING AND CLEANING

Cell No.	Maximum Power in Milli-watts
38	24.68
39	39.47
40	31.96
41	40.45
42	34.71
44	33.87
45	40.23
46	41.48
48	24.76

Arithmetic Mean = 34.6233 Standard Deviation = 6.52

Variance = 42.47 Confidence Limit = 5.3129

TABLE 5-2

MAXIMUM POWER OF SOLAR CELL MODULES

JPL Bus Bar Connectors

CELL TYPE: MICROSHEET BEFORE SANDBLASTING

Cell No.	Maximum Power in Milli-watts
49	50.89
50	49.88
51	50.45
52	49.04
53	50.53
54	51.43
55	50.23
56	51.16
58	52.30
59	51.45
60	52.38

Arithmetic Mean = 51.1450 Standard Deviation = 1.31

Variance = 1.73 Confidence Limit = 0.8830

CELL TYPE: MICROSHEET AFTER SANDBLASTING BUT BEFORE CLEANING

Cell No.	Maximum Power in Milli-watts
51	6.70
52	11.00
53	9.81
54	1.44
55	25.59
56	9.86
57	21.25
58	18.34
59	2.93
60	25.28

Arithmetic Mean = 13.2200 Standard Deviation = 8.85

Variance = 78.24 Confidence Limit = 6.6694

TABLE 5-2 Continued

CELL TYPE: MICROSHEET AFTER SANDBLASTING AND CLEANING

Cell No.	Maximum Power in Milli-watts
50	30.99
51	28.80
52	31.79
53	34.03
54	36.93
55	36.25
56	32.49
57	33.45
58	35.60
59	36.67
60	30.39

Arithmetic Mean = 33.3990 Standard Deviation = 2.76

Variance = 7.60 Confidence Limit = 1.9422

CELL TYPE: FUZED QUARTZ BEFORE SANDBLASTING

Cell No.	Maximum Power in Milli-watts
61	51.06
62	46.54
63	49.03
64	50.73
65	50.43
66	48.00
67	48.95
68	46.05
69	53.42
70	52.91
71	53.68
72	49.81

Arithmetic Mean = 50.0499 Standard Deviation = 2.51

Variance = 6.30 Confidence Limit = 1.6864

TABLE 5-2 Continued

CELL TYPE: FUZED QUARTZ AFTER SANDBLASTING BUT BEFORE CLEANING

Cell No.	Maximum Power in Milli-watts
63	9.40
64	8.55
65	26.35
66	1.30
67	28.08
68	13.91
69	22.56
70	20.17
71	20.29
72	4.25

Arithmetic Mean = 15.4860 Standard Deviation = 9.35

Variance = 87.42 Confidence Limit = 7.0500

CELL TYPE: FUZED QUARTZ AFTER SANDBLASTING AND CLEANING

Cell No.	Maximum Power in Milli-watts
62	27.95
63	29.99
64	30.40
65	31.04
66	36.22
67	36.11
68	30.06
69	31.61
70	32.16
71	34.35
72	35.55

Arithmetic Mean = 32.3127 Standard Deviation = 2.82

Variance = 7.96 Confidence Limit = 1.9881

TABLE 5-2 Continued

CELL TYPE: SAPPHIRE BEFORE SANDBLASTING

Cell No.	Maximum Power in Milli-watts
73	50.82
74	50.71
75	50.79
76	51.86
77	51.60
78	51.69
79	49.93
80	52.18
81	52.32
84	49.78

Arithmetic Mean = 51.1679 Standard Deviation = 0.90

Variance = 0.81 Confidence Limit = 0.6782

CELL TYPE: SAPPHIRE AFTER SANDBLASTING BUT BEFORE CLEANING

Cell No.	Maximum Power in Milli-watts
75	15.25
76	14.28
77	25.53
78	5.58
79	23.01
80	6.02
81	25.83
82	25.33
83	23.93
84	25.91

Arithmetic Mean = 19.0670 Standard Deviation = 8.18

Variance = 66.93 Confidence Limit = 6.1685

TABLE 5-2 Continued

CELL TYPE: SAPPHIRE AFTER SANDBLASTING AND CLEANING

Cell No.	Maximum Power in Milli-watts
74	34.34
75	40.42
76	31.86
77	34.71
78	41.32
79	35.21
80	37.78
81	33.99
82	35.33
83	38.78
84	30.93

Arithmetic Mean = 35.8790 Standard Deviation = 3.33

Variance = 11.10 Confidence Limit = 2.3471

CELL TYPE: INTEGRAL BEFORE SANDBLASTING

Cell No.	Maximum Power in Milli-watts
85	47.36
86	48.91
87	40.68
88	47.67
89	48.94
90	42.85
91	47.31
93	45.40
94	46.07
95	41.73
96	41.15

Arithmetic Mean = 45.2790 Standard Deviation = 3.13

Variance = 9.81 Confidence Limit = 2.2070

TABLE 5-2 Continued

CELL TYPE: INTEGRAL AFTER SANDBLASTING BUT BEFORE CLEANING

Cell No.	Maximum Power in Milli-watts
87	28.25
88	15.41
90	8.58
91	27.38
92	8.81
93	23.62
94	21.45
95	1.47
96	24.67

Arithmetic Mean = 17.7378 Standard Deviation = 9.58

Variance = 91.69 Confidence Limit = 7.8070

CELL TYPE: INTEGRAL AFTER SANDBLASTING AND CLEANING

Cell No.	Maximum Power in Milli-watts
88	37.32
89	33.63

Arithmetic Mean = 35.4750 Standard Deviation = 2.61

Variance = 6.81 Confidence Limit = 10.4373

TABLE 5-3

MODULES USED IN TESTS

Environment	A	B	C	D	Type of Connectors
24 hrs., 50 km/hr., ambient T.	2 50	13 62	25 74	37 86	Silver mesh JPL bus bar
72 hrs., 50 km/hr., ambient T.	3 52	14 64	26 76	38 88	Silver mesh JPL bus bar
24 hrs., 100 km/hr., ambient T.	4 54	15 66	27 78	39 90	Silver mesh JPL bus bar
72 hrs., 100 km/hr., ambient T.	5 51	16 63	28 75	40 87	Silver mesh JPL bus bar
24 hrs., 50 km/hr., 245°K	6 49	17 61	29 73	41 85	Silver mesh JPL bus bar
72 hrs., 50 km/hr., 245°K	9 55	20 67	32 79	44 91	Silver mesh JPL bus bar
24 hrs., 100 km/hr., 245°K	11 58	22 70	34 82	46 94	Silver mesh JPL bus bar
72 hrs., 100 km/hr., 245°K	8 60	19 72	31 84	43 96	Silver mesh JPL bus bar
24 hrs., 50 km/hr., diurnal cycle	10 56	21 68	33 80	45 92	Silver mesh JPL bus bar
72 hrs., 50 km/hr., diurnal cycle	7 57	18 69	30 81	42 93	Silver mesh JPL bus bar
24 hrs., 100 km/hr., diurnal cycle	1 59	24 71	36 83	48 95	Silver mesh JPL bus bar
72 hrs., 100 km/hr., diurnal cycle	12 53	23 65	35 77	47 89	Silver mesh JPL bus bar

A = Corning No. 0211 microsheet

B = fused silica

C = sapphire

D = integral covering

SECTION 6

SUMMARY, CONCLUSIONS, AND RECOMMENDATIONS

6.1 SUMMARY AND CONCLUSIONS

A series of tests was run under simulated Martian environmental conditions to determine the effects of dust storms on the operational efficiency of solar cells. Tests were conducted in specially designed race track-type wind tunnels and in six different environments. Time periods were 24 hours or 72 hours. In each test four modules were used. They differed only in the type of protective cover glass. In order to determine the relative merits of two types of electrical interconnectors, expanded silver mesh and JPL bus bars, each test was repeated with a second set of modules but with different type interconnectors.

The six environments were: (1) wind velocity 50 km/hr., ambient temperature, (2) wind velocity 100 km/hr., ambient temperature, (3) wind velocity 50 km/hr., 245°K, (4) wind velocity 100 km/hr., 245°K, (5) wind velocity 50 km/hr., diurnal temperature cycle 210°K - 305°K, and (6) wind velocity 100 km/hr., and diurnal temperature cycle 210°K - 305°K.

Output of solar cell modules under standardized light conditions was measured, (1) on the virgin cells prior to subjection to dust storms, (2) after dust storms but prior to cleaning and (3) after removing the dust layers. By

this procedure it was possible to determine changes in output due to dust cover and damage, and those due to damage alone.

Amount of damage to cover glasses was determined by microscopic examination of assemblages prior to and after each test. Damage was categorized into pitting, cracking, chipping, and loosening of cover glasses.

In all six environments dust accumulated on all types of modules almost instantaneously. There were no significant differences in amount and character of dust cover which accumulated over periods of 24 hours or 72 hours.

Reduction in power output due to accumulation of dust on modules and damage ranged between 60% and 80%. Permanent damage was responsible for reduction in power output of from 25% to 40%.

Damage of cover glasses due to impact of wind-driven particles which produced pits or miniature craters varied with the material and can be summarized as follows:

Fused silica - very great
Microsheet - moderate
Integral - moderate
Sapphire - minimal

Two types of cover glasses were cracked and chipped to a considerable extent during the dust storms. 56.1% of the microsheet cover glasses were cracked and 22.7% of those of sapphire. There were some indications that cracking was greater in those cover glasses which had been subjected to low temperatures or the diurnal cycle. It must be pointed out, however, that the microsheet cover glass with the greatest crack damage was one that had been tested at ambient temperature.

Unbonding of sapphire and microsheet cover glasses during tests was considerable, particularly in the case of sapphire.

The results of these tests indicate that solar cells are an unreliable source of power during and after subjection to dust storms, such as probably occur on Mars. The accumulation of dust layers and damage to the cover glasses result in drastic reductions of power output. Of the four types of covering material the integral appears to be the best and sapphire in second place. Fused silica and Corning No. 0211 microsheet are unsatisfactory.

There was no serious damage to either type of interconnector, expanded silver mesh, or JPL bus bar. Minor damage due to abrasion and some fraying of the silver mesh was noted

during microscopic examinations. The JPL bus bar probably is the more reliable of the two types.

6.2 RECOMMENDATIONS

If solar cells are to be used as a source of power to operate equipment and apparatus on the surface of Mars, we recommend that banks of additional cells be provided which would take care of a drop in power of 75%. The possibility of using other power sources which can be positioned within the space vehicle and thus protected from dust storms should be investigated. Also, it is recommended that all items of equipment which are to operate in the open on the surface of Mars be tested in wind storm environments and vulnerable areas properly protected.

If solar cells are to be used, we recommend the use of integral covering material as first choice and sapphire cover glasses as second choice. Also, we recommend the use of the JPL bus bar interconnectors.

References

Adams, J. B., 1968, Lunar and Martian surfaces; petrologic significance of absorption bonds in the near infrared: Science, v. 159, p. 1453-1455.

Binder, A. B., and Cruikshank, D. P., 1964, Comparison of the infrared spectrum of Mars with the spectra of selected terrestrial rocks and minerals: Comm. Lunar Planet., v. 2, p. 193-196.

de Vaucouleurs, G., 1954, Physics of the planet Mars: London, Faber and Faber.

Dollfus, A., 1961, Visual and photographic studies of the planets at the Pic du Midi, Chapter 15 in Planets and satellites, Vol. III of the Solar System; Kuiper, G. P., and Middlehurst, B. M., Editors; Chicago, Univ. of Chicago Press.

Gifford, F., 1964, A study of Martian yellow clouds that display movement; Mon. Weather Rev., v. 92, p. 435-440.

Loomis, A. A., 1967, Stability of iron oxides on Mars: oral presentation at Caltech Mars Seminar, Pasadena, Calif.

Maginni, M., 1939, Il Planeta Marte: Milan, Italy, Ulrico Hoepli, Editore-Librario della Real Casa, 400.

O'Leary, B. T., 1967, Mars: visible and infrared studies and the composition of the surface: Berkley, Calif., U. of Calif., dissertation.

Sinton, W. M., 1967, On the composition of Martian surface materials: Icarus, v. 6, p. 222-228.

Slipher, E. C., 1962, Mars, the photographic story: Cambridge, Mass., Sky Publ. Corp., and Flagstaff, Ariz., Northland Press.

Younkin, R. L., 1966, A search for limonite near-infrared spectral features on Mars: Astrophys. J., v. 144, p. 809-818.